NASA CONTRACTOR REPORT

DESIGN OF TWO ELECTROMAGNETIC PUMPS

by G. E. Diedrich and J. W. Gahan

Prepared by
GENERAL ELECTRIC COMPANY
Cincinnati, Ohio
for Lewis Research Center

NATIONAL AERONAUTICS AND SPACE ADMINISTRATION • WASHINGTON, D. C. • NOVEMBER 1967

NASA CR-911

DESIGN OF TWO ELECTROMAGNETIC PUMPS

By G. E. Diedrich and J. W. Gahan

Prepared under Contract No. NAS 3-8500 by
GENERAL ELECTRIC COMPANY
Missile and Space Division
Cincinnati, Ohio

for Lewis Research Center

NATIONAL AERONAUTICS AND SPACE ADMINISTRATION

For sale by the Clearinghouse for Federal Scientific and Technical Information
Springfield, Virginia 22151 – CFSTI price $3.00

FOREWORD

The work described herein was performed by the General Electric Missile and Space Division under NASA Contract NAS 3-8500 to design three electromagnetic pumps for possible use as boiler feed pumps in Rankine cycle, space electric power systems. Mr. James P. Couch of the Space Power Systems Division, NASA-Lewis Research Center, was the Technical Manager.

ABSTRACT

A design study program initiated by NASA to determine three specific EM pump designs for possible use as boiler feed pumps in Rankine-cycle, space electric power systems is described. The three designs were:

1) 9 lb/sec, 240 psi pump for 1000°F potassium using a T-111 duct
2) 9 lb/sec, 240 psi pump for 1000°F potassium using a 316 SS duct
3) 3.25 lb/sec, 240 psi pump for 1000°F potassium using a T-111 duct

A specific design for each of these ratings is described in detail. Complete calculated performance and evaluation for each design is also presented.

Final design selection for each rating was based on efficiency, reliability, weight and fabricability. In general, efficiency was optimized.

CONTENTS

ILLUSTRATIONS

TABLES

NOMENCLATURE

Units are not indicated since relationships used are valid in any consistent system of units. Units are indicated where numerical values are given in the report.

A	area
B	magnetic induction (magnetic flux density)
c	length of fluid passage in duct
C_p	specific heat
D_h	hydraulic diameter
g	length of magnetic gap; gravitational acceleration
h	hydraulic loss factor as a number of velocity heads
I_l	phase current
N_H	Hartmann number
N_R	Reynolds number
P	pressure
q	heat flow rate
Q	fluid flow rate
R	resistance (electrical)
s	slip
T (ΔT)	temperature (change in temperature)
v	velocity of fluid
V_l	phase voltage
KW	power (kilowatts)
X	reactance
δ	friction factor
μ	fluid viscosity
ρ	electrical resistivity of fluid
σ	weight density of fluid

Subscripts

c	pertaining to stator can or coolant in heat exchanger
d	pertaining to the duct
f	pertaining to the fluid
g	pertaining to the magnetic gap
h	hydraulic, harmonic
i	pertaining to magnetic iron
m	pertaining to magnetic path, magnetization or mutual
ti	pertaining to thermal insulation
1	pertaining to the stator winding or duct wrapper
2	pertaining to the helical duct

I. SUMMARY

A design study program to determine the feasibility and suitability of using electromagnetic pumps as the boiler feed pumps in Rankine-cycle space electric power plants has been performed. A specific application involving three different designs was considered.

Reference 1 evaluates several types of EM pumps for space applications. Based on the conclusions reached in Reference 1 and the specific ratings considered in the present study (i.e., relatively low flow and high pressure), a three phase helical induction type EM pump was selected. For the ratings required, the helical EM pump is extremely reliable, has low weight and can be designed for relatively high efficiency and overall good performance. Several design concepts and arrangements for the basic helical induction EM pump were evaluated. The particular design concept selected, based on reliability and feasibility, consists of a canned, hermetically sealed stator filled with an inert-gas heat-transfer medium, and a completely sealed duct environment, also filled with inert gas. This results in a completely sealed pump with the stator region isolated from the duct region by a thin can in the stator bore which prevents outgassing products from the stator from reaching the pump duct.

Three helical induction EM pump designs were optimized to meet design point requirements. These designs were selected primarily on the basis of efficiency, fabricability and weight. Efficiency was optimized insofar as possible. These designs have relatively high efficiency and low weight compared to previously built commercial EM pumps.

One optimum design is a helical induction electromagnetic pump rated at 3.25 lb/sec (32.8 gpm), 240 psi developed head, 1000°F potassium with 7 psi net positive suction head. This pump is capable of operating continuously at its rated point with an efficiency of 20 percent. It is also capable of operation over a range of temperatures from 900° to 1300°F, a range of flows from 1.5 lb/sec to 4.25 lb/sec and at developed pressures up to 250 psi. The final design is based upon an NPSH of 7 psi at the rated point although within certain limitations of flow it can operate at an NPSH as low as 3 psi. Other performance characteristics of this pump are listed in Table 1.

A helical induction EM pump rated at 9 lb/sec (90.7 gpm), 240 psi developed pressure, 1000°F potassium with 7 psi NPSH was also designed. This design used a T-111 duct, but a 316 stainless steel duct was also designed as an alternate arrangement. Performance characteristics for both ducts at this design point are listed in Table 2.

These designs utilize high temperature structural, electrical, magnetic and insulation materials to permit operation of the complete pump at temperatures above 600°F. The electromagnetic stator is cooled with NaK at 600-700°F and is designed to operate at temperatures up to 1000°F by using nickel-clad silver wire, Hiperco 27 magnetic material and a completely inorganic electrical insulation system. The duct can handle potassium up to 1300°F and is made of T-111 alloy refractory metal.

Complete design layouts and calculated performance characteristics for each design are presented. Detailed descriptions of the designs as well as many of the detailed calculations and a discussion of the performance and several design parameters are also included.

II. INTRODUCTION

An extensive research program investigating all types of EM pumps for several different space applications was reported in Reference 1. In addition, many commercial EM pumps have been developed, designed and built for liquid metal test facility loops and sodium cooled nuclear power plants. All these pumps have exhibited excellent reliability and performance. Extensive development work has also been done on high temperature materials for use in space applications as reported in References 2 through 6. Based on this background it appears feasible to consider the use of EM pumps for space electric power systems provided the efficiency can be improved and weight reduced compared to the commercial variety.

To prove feasibility, an analytical design study to determine three practical, optimum EM pump designs for possible use as boiler feed pumps in Rankine-cycle, space electric power systems was conducted. The three specific designs, as identified by their design point characteristics, were as follows:

1) 9 lb/sec flow rate, 240 psi developed head, 1000°F potassium, 7 psi NPSH, using T-111 pump duct material.
2) 9 lb/sec flow rate, 240 psi developed head, 1000°F potassium, 7 psi NPSH, using 316 stainless steel pump duct material.
3) 3.25 lb/sec flow rate, 240 psi developed head, 1000°F potassium, 7 psi NPSH, using T-111 pump duct material.

To determine these specific designs and obtain the best balance among weight, reliability and efficiency, several hundred design variations are considered, analyzed and evaluated. The scope of work required also includes complete electrical, mechanical, hydraulic and thermal analysis of the final designs, selection of the basic materials to be used, evaluation and selection of the basic design concept and preparation of design layout drawings which can be used to produce manufacturing drawings.

These final designs represent a basic part of the overall program of applying EM pumps to space electric power plants. The designs determined in this study can be built and tested to confirm their suitability for space applications.

III. DESIGN DESCRIPTION

A. Principle of Operation

In all EM pumps a body force is produced on a conducting fluid by the interaction of an electric current and magnetic field in the fluid. This body force results in a pressure rise in the fluid as it passes from the inlet to the outlet of the EM pump. This body force is analogous to the familiar fundamental principle of force on a current carrying conductor in a magnetic field which is the operating principle of many common electromagnetic devices.

The polyphase helical induction EM pump employs this principle in the same manner as a polyphase induction motor. The pump contains an electromagnetic stator assembly and a duct assembly in the stator bore. When power is applied to the three phase stator winding a revolving magnetic field is produced in the stator bore. This magnetic field induces voltage in the conducting fluid contained in the duct, and as a result of this induced voltage, currents will flow in the fluid. These currents interact with the magnetic field to produce a body force on the fluid causing it to move through the duct thereby developing pressure. The pressure gradient at any point in the fluid is proportional to the product of magnetic field strength and the component of current density perpendicular to magnetic field strength. The total pressure rise developed by the pump is the integral of this pressure gradient over the axial length of flow passages in the pump duct.

B. General Arrangement

The general arrangement for all three specific designs determined in this study is basically the same. Figure 1 is the design layout for the 3.25 lb/sec pump which consists of four major parts: the pump duct, the heat exchanger and frame, the stator and the thermal insulation. Figures 2 and 3 show the 9 lb/sec pumps.

In the configuration shown in Figure 1, flow enters the pump duct through the schedule 10 inlet pipe into a short annular region, then into and through the helical passage where pressure is developed by the electromagnetic body force on the fluid. After leaving the helical passage the fluid flows back through the center return leaving the pump through a schedule 10 outlet pipe at the same end it entered.

In order to permit operation at relatively low NPSH the first two turns of the helical flow passage have a larger cross-section than the remaining turns. In this way low fluid velocity is maintained near the pump entrance where the NPSH is low. As pressure is developed in the helical passage the velocity is increased. After the second turn of the helix the velocity is maintained at a relatively high value for the remainder of the pumping section to permit more efficient pumping.

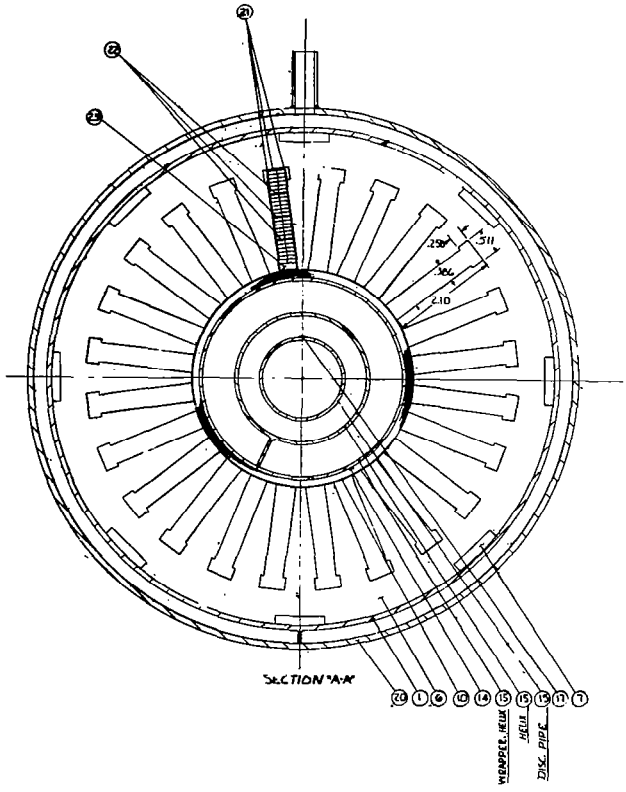

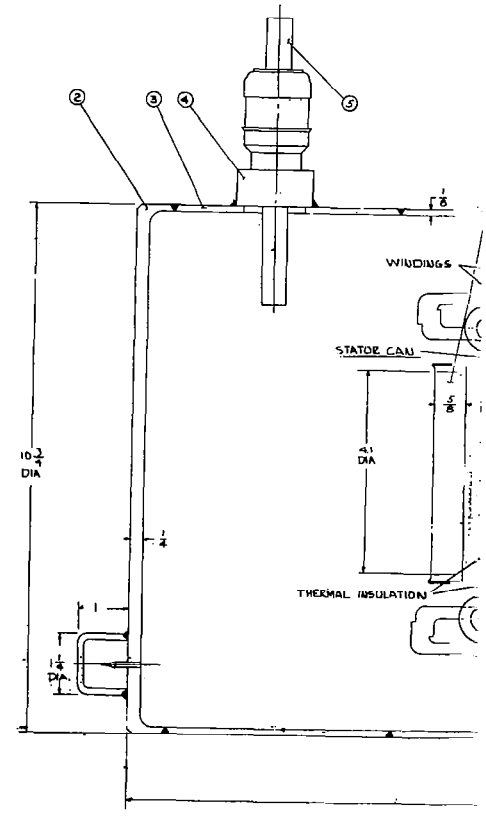

Figure 1. Design Layout (3.

1	HEAT EXCHANGER	HASTELLOY "B"
2	END SHIELD	INCONEL
3	LEAD SEAL SUPT. RING	INCONEL
4	LEAD SEAL SUPT. FL	INCONEL
5	STUD, TERMINAL	NICKEL
6	CORE, STATOR	HYPERCO-27
7	BAR, BUILDING	CARBON STL
8	WELDING RING	CARBON STL
9	WINDING, COND	Ni CLAD Ag
	WDG. INSUL. STRD	DBL LAYER ALNADUR
10	CAN, STATOR	INCONEL
11	END PLATE	INCONEL
12	SEAL RING	INCONEL
13	SEAL RING FLG.	T-111 ALLOY
14	INSULATION	Cb-1Zr FOIL
15	DUCT	T-111 ALLOY
16	CORE-CENT. IRON	HYPERCO-27
17	KEY	HYPERCO-27
18	DOWEL	HASTELLOY "B"
19	WELDING RING	T111 ALLOY
20	WRAPPER, HEAT EX.	HASTELLOY "B"
21	SLOT LINER	ALUMINA
22	SEPARATOR	ALUMINA
23	WEDGE	ALUMINA
24	SPACE BLOCKS	CARBON STL
25	EVACUATION TUBE	INCONEL
26	CAP, EVAC. TUBE	INCONEL

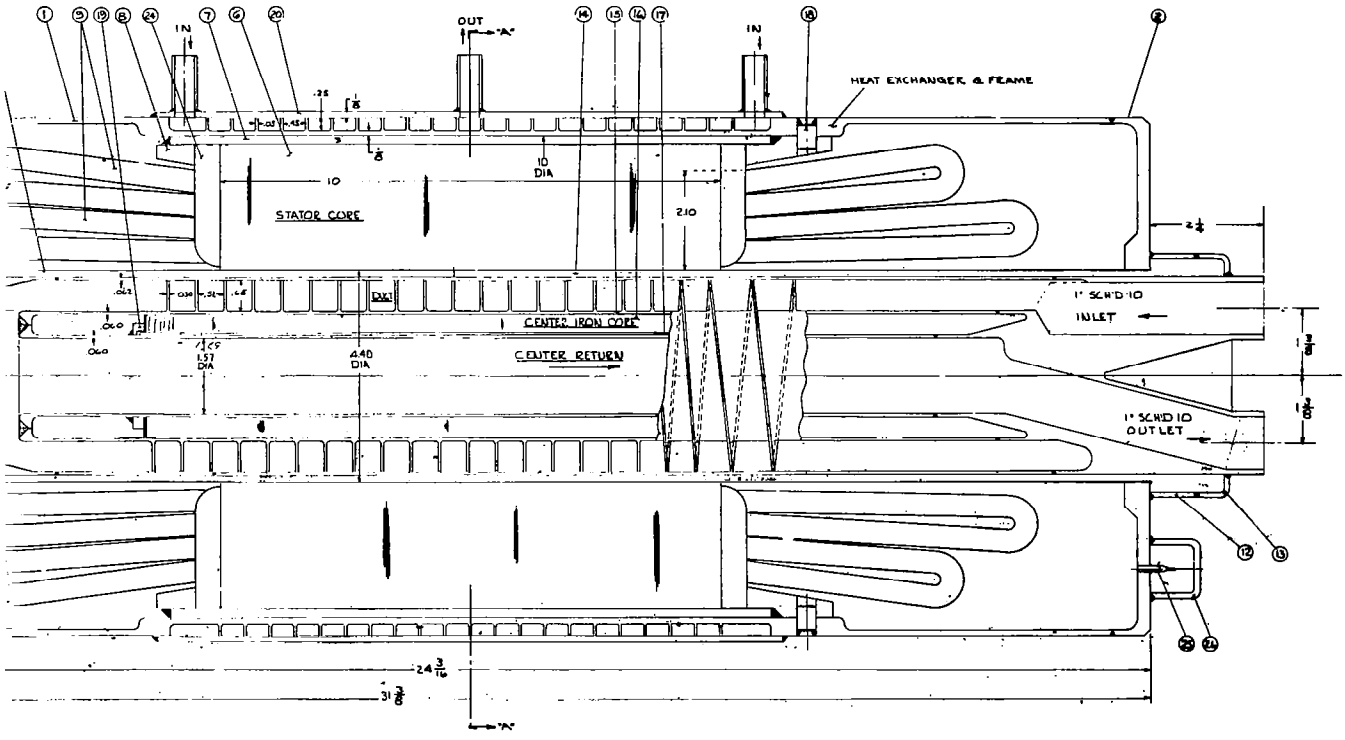

P1092-1

/sec Pump, T-111 Duct).

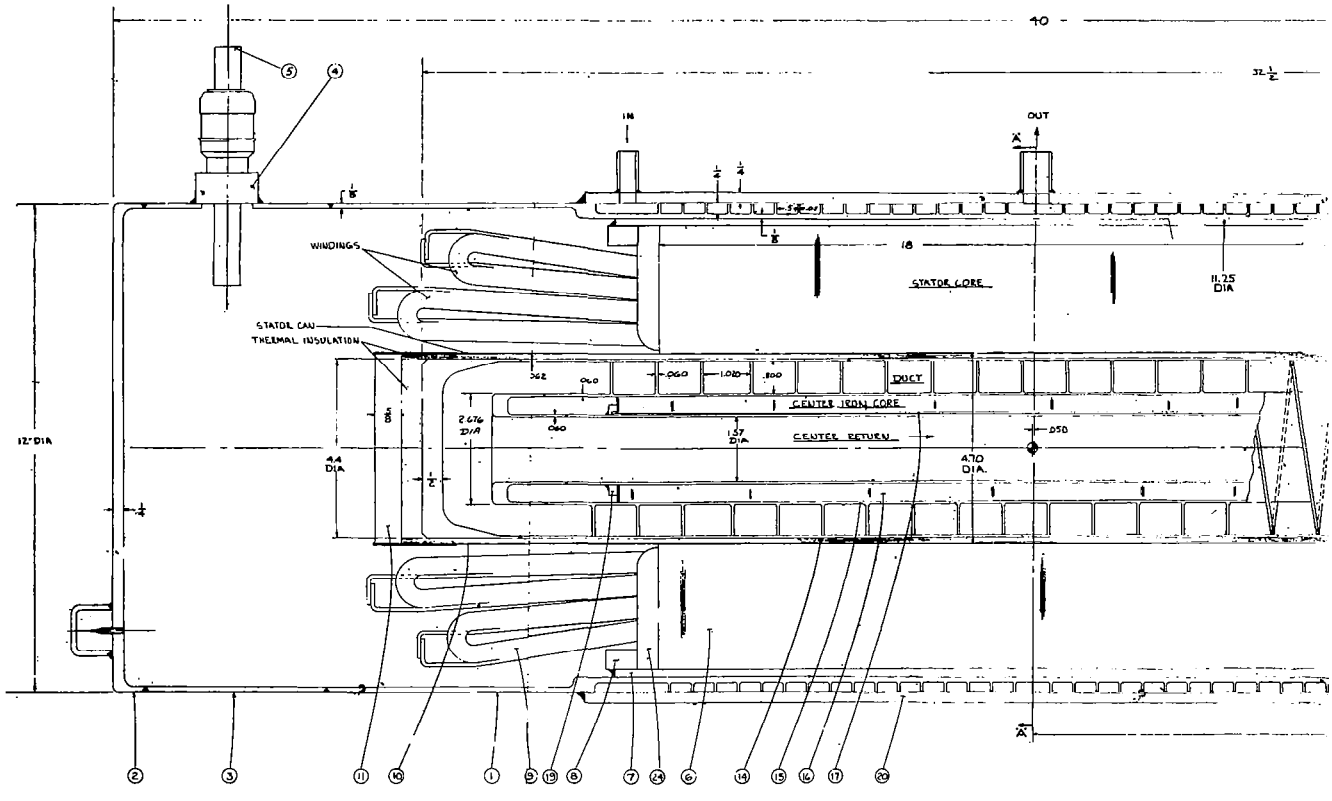

Figure 2. Design Layout (9 lb/s

LIST OF MATERIALS		
PC*	DESCRIPTION	MAT'L
1	HEAT EXCHANGE	HASTELLOY "B"
2	END SHIELD	INCONEL
3	LEAD SEAL SUPPORT	INCONEL
4	LEAD SEAL SUPT FL.	INCONEL
5	STUD, TERMINAL	NICKEL
6	CORE, STATOR	HYPERCO-27
7	BAR, BUSLOOP	CARBON STL
8	WELDING RING	CARBON STL
9	WINDING, COND.	U. CLAD Ag
	WINDING, TERM. STUDS	DBL LAYER ARMOUR
10	CAN, STATOR	INCONEL
11	END PLATE	INCONEL
*12	SEAL RING	INCONEL
13	SEAL RING, FLANGE	T-111 ALLOY
14	INSULATION	Cb 1% Zr FOIL
15	DUCT	T-111 ALLOY
16	CORE CENT. RING	HYPERCO-27
17	KEY	HYPERCO-27
18	DOWEL	HASTELLOY "B"
19	WELDING RING	T-111 ALLOY
20	WRAPPER, HEAT EXC.	HASTELLOY B*
21	SLOT LINER	ALUMINA
22	SEPARATOR	ALUMINA
23	WEDGE	ALUMINA
24	SPACE BLOCKS	CARBON STL
25	CONCENTR TUBE	INCONEL
26	CAP, EXC. TUBE	INCONEL

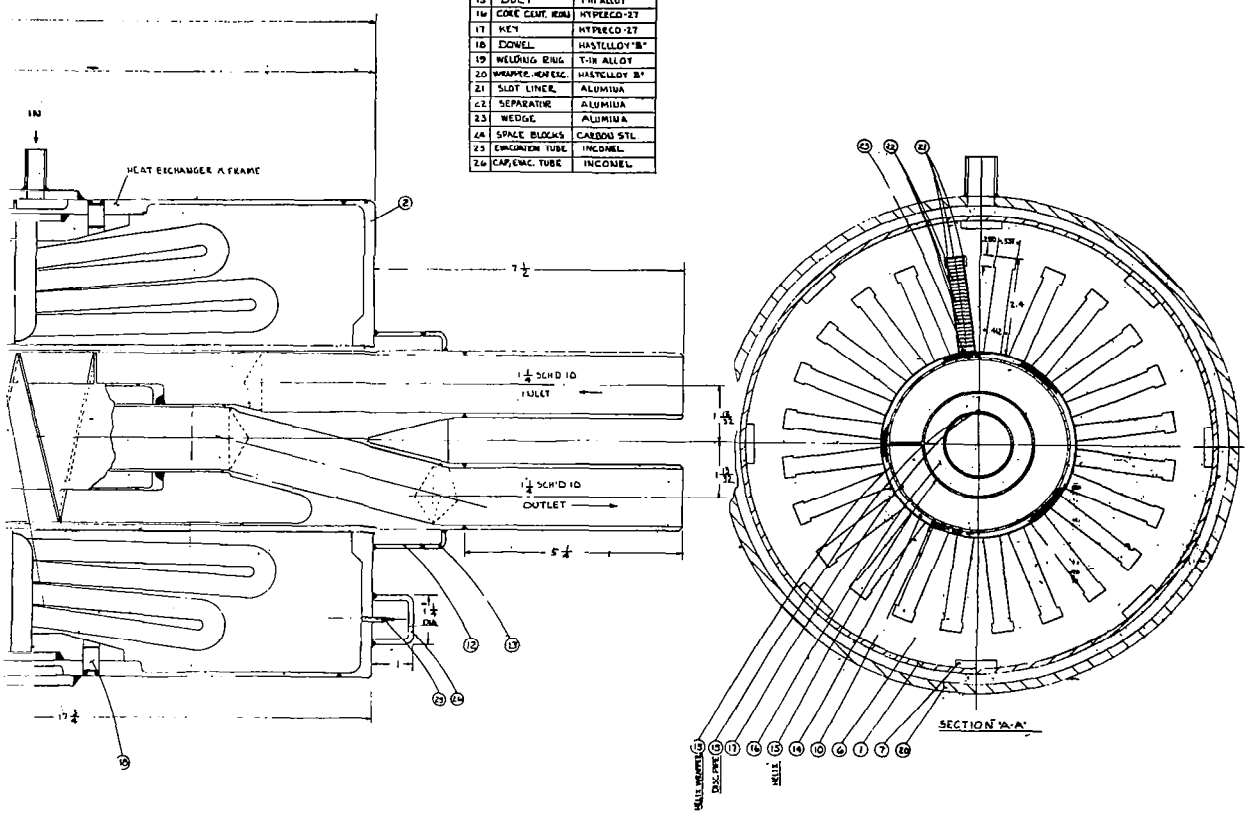

imp, T-111 Duct).

P1092-2

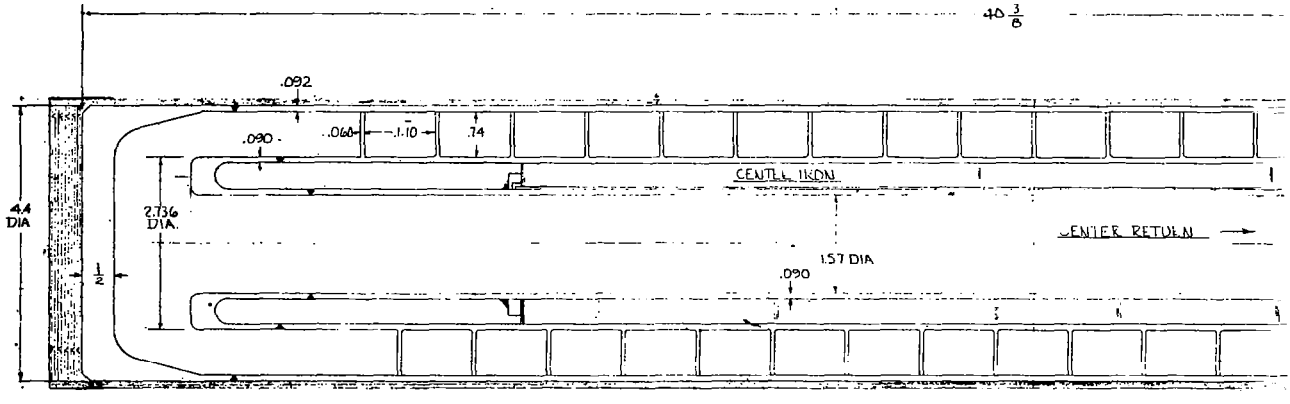

Figure 3. Design

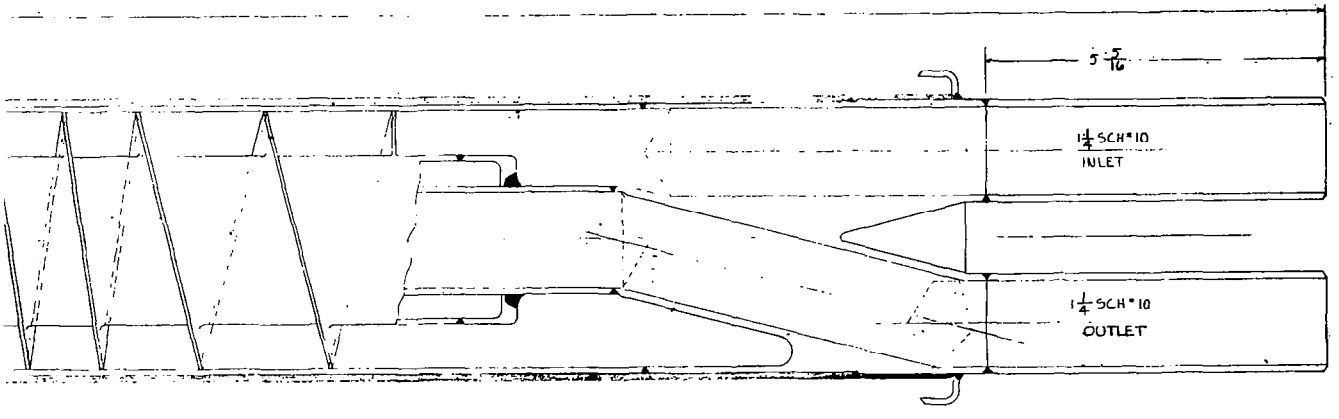

ut (316 SS Duct).

P1092-3

The pump is cooled by means of a heat exchanger around the periphery of the pump frame. The heat exchanger consists of a machined helical passage with an inlet pipe at each end and an outlet pipe at the center of the pump frame region adjacent to the stator. Heat is conducted from the windings through the stator core to the frame where the heat is removed by circulation of liquid metal coolant through the heat exchanger.

The stator core and windings are completelyenclosed and sealed by the frame, end shields and a thin can inside the stator bore. This enclosed stator region will be filled with an inert gas to facilitate heat transfer between the windings and the stator laminations and on to the frame. Electrical power is transmitted to the stator windings through hermetic lead seals in the pump frame. The thin can, besides sealing the stator cavity region, acts as a protective shield to prevent outgassing products from the stator from reaching the duct.

The region between the duct and the stator can contains thermal insulation consisting of several layers of rippled metallic foil. This region is sealed from the outside environment by a bimetallic sleeve at the inlet/outlet end welded between the end shield and the duct. By sealing this region, secondary back-up is provided for the stator can which is an additional reliability feature of the design. This space between the duct and stator can is also filled with an inert gas to approximately the same pressure as the gas in the stator region.

C. Stator Assembly

The stator consists of a laminated punching stack and form-wound coils arranged to form a two pole magnetic field revolving at 60 revolutions per second, three phase power. Selection and evaluation of the specific electrical, magnetic and insulating materials for the stator assembly were based primarily on prior development work done under government contract. The results of this work and the data generated are contained in References 2 through 6.

The punching stack consists of magnetic laminations which provide a low reluctance path for the magnetic flux as in a conventional induction motor stator. The strength requirements for the stator laminations are not severe. Since the frequency is relatively low (60 cps), low loss is not essential either. The main requirement is that the material maintain its highly magnetic characteristics at its operating temperature which will be between 700°F and 900°F. The magnetic material for these laminations will be Hiperco 27 approximately 0.025 inches thick. For the conditions of operation and in this lamination thickness, Hiperco 27 has excellent magnetic characteristics, good thermal conductivity and reasonably low loss. Each lamination contains 24 slots for the stator winding.

Interlaminar insulation is provided by a plasma sprayed alumina coating on each lamination. This coating will be approximately 0.001 to 0.002 inches thick.

The stator cores for each 9 lb/sec pump are identical; the core for the 3.25 lb/sec pump is very similar, being different only in certain dimensions. A comparison of the important dimensions is as follows:

	9 lb/sec pump	3.25 lb/sec pump
Core length	18"	10"
Bore diameter (punching)	4.4"	4.1"
Outside diameter (punching)	11.25"	10"
Slot width	.412"	.386"
Slot depth	2.4"	2.1"

These dimensions, among others, are shown in Figures 1, 2, 3, 6 and 7.

The stator laminations are held together by 8 building bars of rectangular cross-section spaced uniformly around the outer periphery of the punching stack and welded at each end to a welding ring to form a tightly compressed stack of laminations. The stator core has an interference fit at its outer periphery with the pump frame thereby insuring good heat transfer from the stator to the heat exchanger. In addition, two dowel pins are inserted through the frame into one of the welding rings to properly position the stator core.

Form wound coils are inserted in the 24 slots of the stator core. The conductor material will be nickel-clad silver wire having a conductor cross-section area of 20% nickel. This conductor material has an acceptable electrical conductivity at the operating temperature range of 900°F to 1000°F. The electrical conductivity of this conductor material is one of the major factors contributing to the relatively high pump efficiency. Other considerations given to conductors for high temperature operation include thermal conductivity, physical strength, creep and rupture strength, resistance to oxidation both during processing and normal operation, thermal diffusion stability, and the ease with which joint fabrication and other manufacturing processing can be accomplished. The nickel-clad silver conductor meets the additional considerations cited within the limitations now defined. At some future time, after the thermal cycling requirements have been established, the creep and rupture fatigue properties must be reappraised in the light of the thermal cyclings requirements.

The conductor insulation will be an Anadur coating, except that an "S" glass will be used in lieu of an "E" glass. The "S" glass will provide higher physical properties for the temperature range of 900°F to 1000°F. Specifically, a double Anadur coating will be used; this is consistent with the design practice applied to motors for industrial, utility, and special applications where double glass served conductors are used in lieu of single glass served conductors.

The slot insulation, coil layer separators, and slot wedges will be high purity, 99.5 percent or greater, alumina which has been solid molded. These are delineated in Figures 4 and 5. The slot insulation will consist of three pieces, a bottom U-shaped piece and two side sheets as shown in these figures. A one piece U-shaped slot tube is not feasible from a manufacturing and handling standpoint. The slot insulation and separators will be approximately 0.025 inches thick while the wedges will be 1/8 inches to 3/16 inches thick in each design.

The coils can be inserted into the stator core to form either a single layer or double layer winding arrangement as shown in Figure 6 for the 3.25 lb/sec design and Figure 7 for the 9 lb/sec design. For comparison these figures show one coil inserted in appropriate slots for the single layer winding pattern and two coils inserted in appropriate slots for the double layer winding pattern. The complete double layer winding arrangement contains twice as many individual coils, each coil having only half as many turns, compared to the single layer winding arrangement. From a performance standpoint the two arrangements are equivalent. The design layouts shown in Figures 1 and 2 were made using the double layer coil arrangement. The single layer arrangement does not change any of the significant dimensions in these figures, only the delineation of the winding.

The coil cross-sections as established in this design study are shown in Figures 4 and 5 which are drawn for the double layer coil arrangement. For the 9 lb/sec designs each coil consists of four turns (2 turns double layer) of rectangular wire, 0.075" x 0.165" six wires in hand, each strand insulated with a double coating of Anadur. Each coil of the 3.25 lb/sec design consists of four turns (2 turns double layer) of rectangular wire, 0.063" x 0.150" six wires in hand, each strand insulated with a double coating of Anadur. The complete stator winding consists of twenty-four coils (48 coils if double layer winding arrangement is used), each coil spanning ten teeth thereby giving 5/6 pitch. The stator winding has 32 turns in series per phase and is connected in a 1 circuit, 3 phase delta-connection for the 9 lb/sec pump and 1 circuit 3 phase Y - connection for the 3.25 lb/sec pump.

The final decision on specific coil arrangement, the final coil and insulation geometry, the need and choice of a winding impregnating material and coil end bracing must be appraised and evaluated based on the physical characteristics of the materials involved; e.g., the handling characteristics of the wire.

D. Heat Exchanger and Frame

Surrounding the stator core is the pump heat exchanger and frame. Liquid metal coolant, NaK, is circulated through the helical passage in the heat exchanger to remove heat conducted from the windings through the stator core.

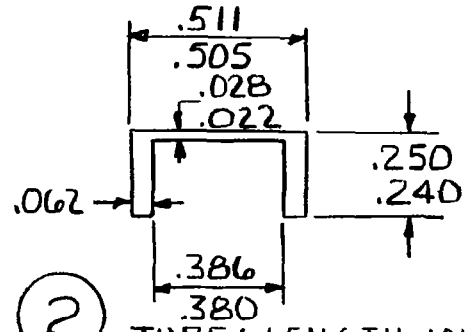

(2) TUBE: LENGTH = 10"
MAT'L: 99.5% ALUMINA
SOLID MOLDED

(1) SHEET:
HEIGHT = 2.075
LENGTH = 10"
THICKNESS = .022-.028
MAT'L: 99.5% ALUMINA
SOLID MOLDED

(3) SEPARATOR:
THICKNESS: .022-.028
WIDTH: .324-.327
LENGTH: 10"
MAT'L: 99.5% ALUMINA
SOLID MOLDED

(4) WEDGE:
THICKNESS = .136-.142
WIDTH = .324-.327
LENGTH = 5"
MAT'L = 99.5% ALUMINA
SOLID MOLDED

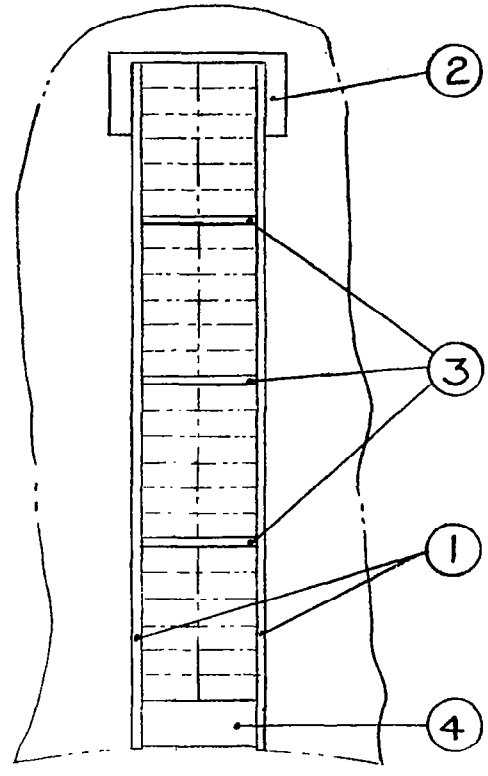

P1092-4

Figure 4. Slot Insulation (3.25 lb/sec Pump)

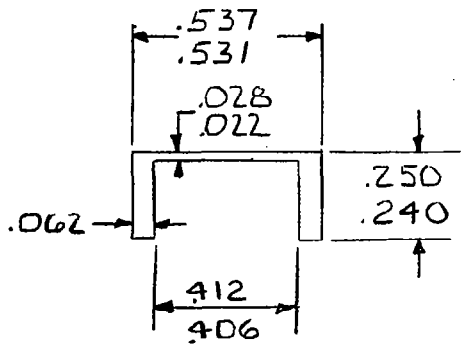

(2) TUBE:
LENGTH = 18"
MAT'L: 99.5% ALUMINA
SOLID MOLDED

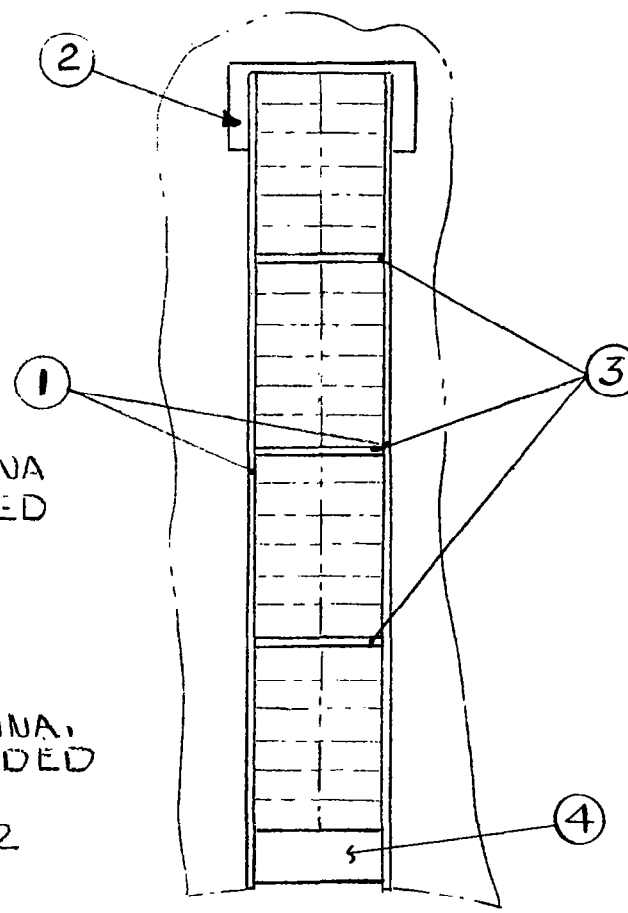

(1) SHEET:
HEIGHT = 2.375
LENGTH = 18"
THICKNESS = .022-.028
MAT'L: 99.5% ALUMINA
SOLID MOLDED

(3) SEPARATOR:
THICKNESS = .022-.028
WIDTH = .350-.353
LENGTH = 18"
MAT'L = 99.5% ALUMINA,
SOLID MOLDED

(4) WEDGE:
THICKNESS = .136-.142
WIDTH = .350-.353
LENGTH = 4 1/2"
MAT'L = 99.5% ALUMINA, SOLID MOLDED

P1092-5

Figure 5. Slot Insulation (9 lb/sec Pump)

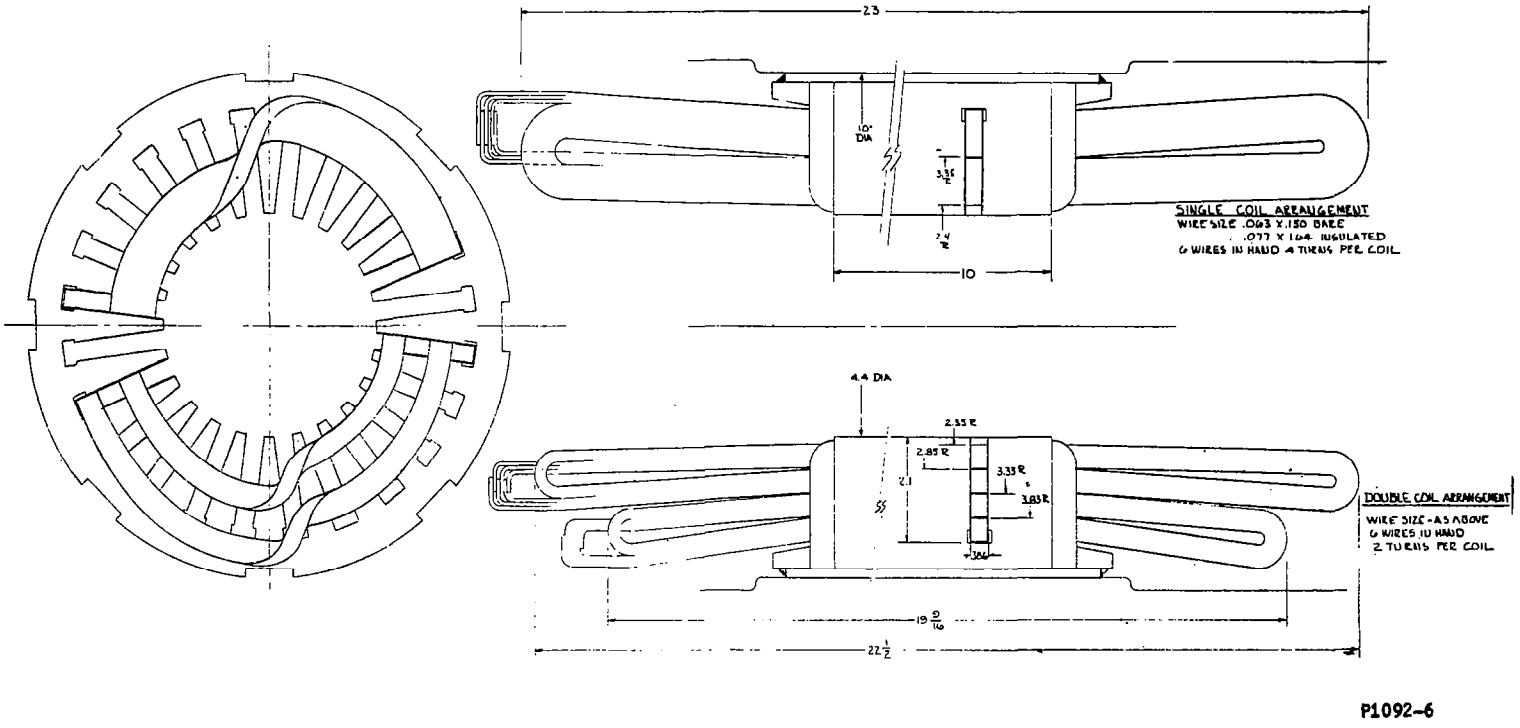

Figure 6. Punching and Coil Layout (3.25 lb/sec Pump).

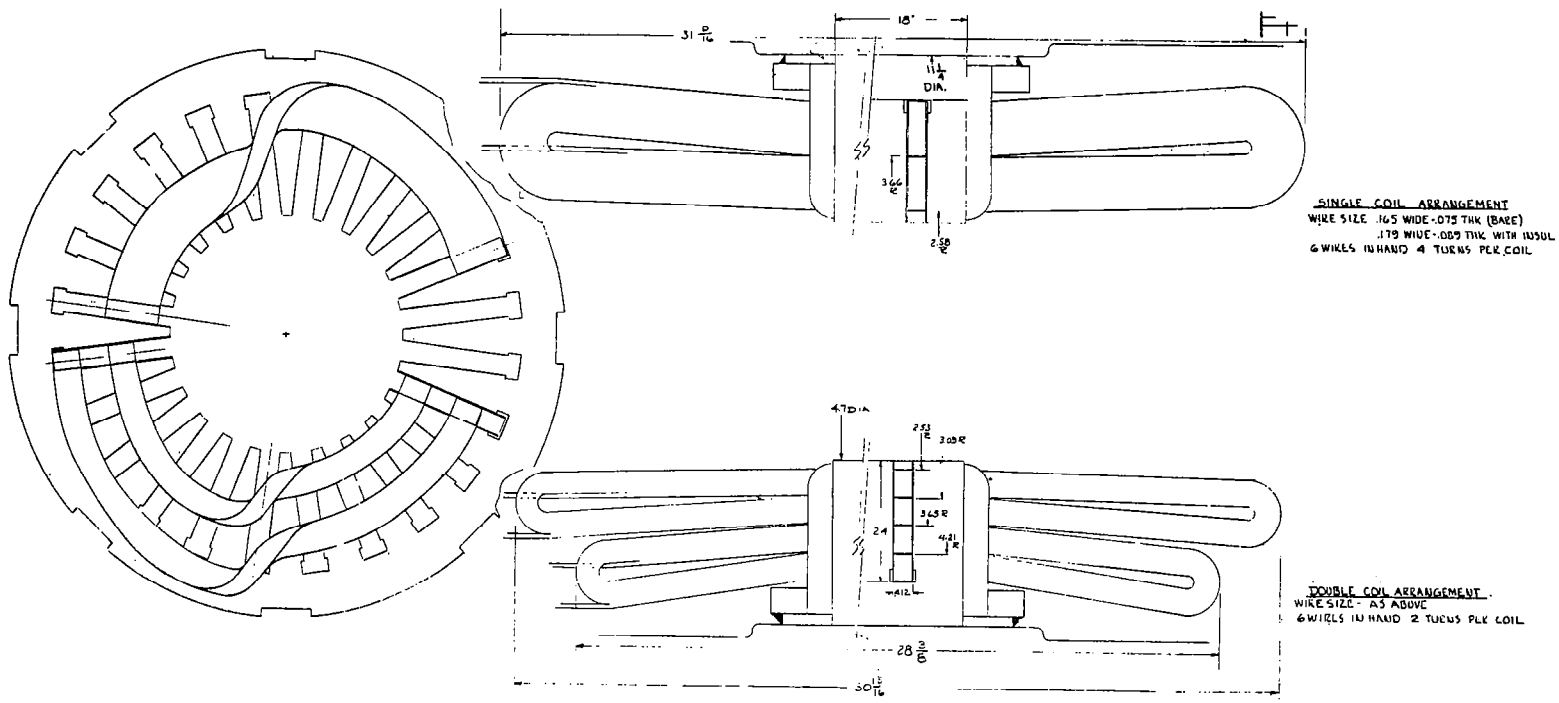

Figure 7. Punching and Coil Layout (9 lb/sec Pump).

The material selected for the pump frame and heat exchanger is Hastelloy B. This material has adequate strength at operating temperature, is a satisfactory containment material for the liquid coolant (NaK) in the heat exchanger and comes quite close to matching the thermal coefficient of expansion of the Hiperco 27 stator core. By matching the thermal expansion of the Hiperco 27 stator core, the interference fit between the heat exchanger and the core is easily maintained. Hence good heat transfer between the core and heat exchanger is assured at operating temperature. Beyond the ends of the heat exchanger, the pump frame material will be Inconel. The end shields and stator can in the stator bore are also Inconel to permit easier fabrication and joining. The heat exchanger, frame, end shields and stator can provide all welded construction and form a completely sealed envelope around the stator assembly. The only penetrations through this envelope will be the hermetic lead seals to transmit power to the stator windings, thermocouple wells to provide means of monitoring stator winding temperature and an evacuation plug to provide a means of leak testing the unit, evacuating the stator region and filling with inert gas. All these penetrations will be completely sealed by brazed or welded joints.

Most of the dimensions for the heat exchanger and frame are shown in Figures 1 and 2.

E. Duct

The T-111 duct for the 9 lb/sec design is shown in Figure 2. Because the allowable design stresses for T-111 are so high at operating temperature, the minimum duct wall thickness is limited by fabrication considerations and material homogeneity rather than by stress considerations. The axial length of the helical duct for this design is approximately 22 inches with the overall length including inlet/outlet connector being about 40 inches. The outside diameter of the duct is 4.4 inches. Cross-sectional dimensions of the machined helical passage are also shown in Figure 2.

The T-111 duct for the 3.25 lb/sec design is delineated in Figure 1. It is similar to the above T-111 duct except its outside diameter is 4.1 inches, axial length of helix is 13 inches and overall length is 31 inches. The flow passage cross-sectional dimensions are also somewhat different and shown in Figure 1.

The 316 stainless steel duct for the 9 lb/sec pump is shown in Figure 3. This duct is interchangeable with the T-111 duct for the 9 lb/sec pump shown in Figure 2; i.e., it has the same outside diameter and overall length and will fit into the same stator bore. Both 9 lb/sec pump designs use the same stator design. Due to stress limitations of stainless steel the wall thicknesses are increased to about 0.090 inches. To accommodate this increase in wall thickness the helical flow passage is more shallow and slightly wider. In this way the same flow passage cross-sectional area and fluid velocity is maintained. Because of the higher electrical resistivity of stainless steel relative to T-111, the electrical losses in the stainless steel duct are less (even though the duct walls are thicker) and hence the overall pump efficiency is slightly higher.

In both the T-111 and 316 stainless steel duct, the first turn of the helical flow passage has a rather large cross-sectional area to permit low fluid velocity at entrance and hence operation at lower NPSH. The cross-sectional area of the second turn gradually changes from this relatively large area to a smaller area which is maintained for the remaining turns of the helical passage. During this second turn the velocity increases to its final, relatively high, value for more efficient pumping during the remainder of the duct. This variable fluid velocity is accomplished in the duct by employing a dual pitch for the helix. The machined helix has a pitch of 1.86 inch for the first two turns and 1.08 inch for the remaining turns in the case of the 9 lb/sec T-111 duct. The 9 lb/sec 316 stainless steel duct has a pitch of 2 inch for the first two turns of the helix and a pitch of 1.16 inch for the remaining turns. The 3.25 lb/sec T-111 duct has a pitch of 0.85 inch for the first two turns and a pitch of 0.57 inch for the remaining turns.

Enclosed between the helical flow passage and the center return pipe is a center iron core. This center iron core consists of magnetic laminations (washers) of Hiperco 27 having the same thickness and same interlaminar insulation as the stator core laminations. These laminations are held together in a tight stack and positioned by a key and ring at each end which is welded to the center return pipe of the duct.

F. Thermal Insulation

The thermal insulation between the duct and stator can consists of several layers of laminated strips of rippled metallic foil. It is recommended that these strips be about 0.5 inch wide by 0.002 inch thick with the ripples being 0.010 inch to 0.015 inch deep. The foil should be Cb-1%Zr (or similar refractory metal) for the T-111 ducts. Stainless steel foil is satisfactory for the 316 stainless steel duct.

The thermal insulation region is sealed by the bimetallic sleeve welded between the end shield and duct as shown in Figures 1 and 2. After assembly this region is to be evacuated and filled with argon.

IV. DESIGN EVALUATION

A. Evolution of Design Concept

The removal of the EM pump heat losses in the space environment requires special design effort and, hence, several design concepts and arrangements for the helical induction EM pump were considered and evaluated.

Two basic design concepts considered were:

1) Gas-filled stators

2) Open-to-space stators

The gas-filled stators use the thermal conductivity of a gas, which fills all the voids between the conductors and the slots and elsewhere in the stator winding cavity, to assist heat conduction from the windings to the heat exchanger. In the open-to-space stators heat transfer is primarily by conduction through solids from the windings to the heat sink, and hence good contact between solids with no voids must be obtained.

Five specific stator cooling arrangements based on these two basic concepts have been investigated from the standpoint of structural feasibility and heat transfer capability. The design evaluation was based on the design point conditions of 240 psi developed head and 9 lb/sec potassium flow at 1000°F entering the pump with a 7 psi net positive suction head.

The five specific arrangements considered were:

1) Hermetically Sealed Designs

   a) Canned Pump

   b) Canned Stator

2) Open-to-Space Designs

   a) Potting Compound Conduction Cooling

   b) Conduction Cooling (Heat Transfer Blocks)

   c) Liquid Metal Cooled Conductors (Conductor Tubing)

Under the grouping of hermetically sealed designs the entire EM pump can be enclosed and filled with an inert gas (canned pump) or the stator cavity only can be canned (canned stator).

In the canned EM pump concept, a hermetically sealed shell enclosure surrounds the entire pump structure. The duct is inserted from one side and

attached to the shell by a collar. An inert gas fills all the voids and cavities between the duct and outer shell. Heat is removed from the winding end turns by conduction along the winding to the stack, then through the stack and shell to the liquid NaK coolant. This concept results in a very rugged, reliable structure.

The canned stator differs from the canned pump design in that two concentric cylinders are sealed at each end to enclose the stator only. The inner cylindrical can is inside the stator bore, and since it lies in the rotating magnetic field, eddy current losses occur in it. In order to keep these losses small, a very thin wall design and a material with high electrical resistivity are chosen for the stator can.

The canned stator requires some additional support structure to maintain the pump duct in its correct position. It is a slightly less reliable design than the thicker walled canned pump, due to the thin stator can being part of the containment for the gas in the stator cavity. However, it has the advantage of isolating the stator region from the duct and thereby preventing outgassing products of the winding from reaching the duct. From the winding and stack heat transfer standpoint, both these arrangements are equivalent because both rely on the thermal conductivity of a gas in the stator cavity at interfaces and voids between solid members.

In open-to-space stators the gas can be replaced by a potting compound. This potting compound is poured into the voids as a liquid and solidifies. It has the advantage of cementing the windings together to form one solid block.

Since most potting compounds have a higher thermal conductivity than gases, better heat transfer from the end turns might result, but this assumes that all voids would be completely filled. As yet, there is no potting compound available, which can fill the voids as adequately as a gas and which has a sufficiently flexible thermal expansion capability to preclude cracking or losing surface contact with the conductor strands and stator core.

The winding conduction cooling arrangement uses the principle of applying positive contact pressure between flat electrical conductor surfaces and flat ceramic plates which act as thermal conductors and electrical insulators. Metal oxides, such as alumina or beryllia, can be used as interfaces for these heat transfer blocks. These metallic oxide interfaces could be thin and of the same order of magnitude as the electrical insulation thickness. The design approach would be to apply such heat transfer blocks locally at the end turns where they can also be used as a winding support structure. Room at each end of the stack around and adjacent to the end turns can be made available for positioning these heat transfer elements.

The present two-pole EM pump design uses several turns per coil. Since the heat losses have to be removed individually from each turn the present winding layout arrangement requires approximately 288 small heat transfer blocks per end.

The heat transfer block winding cooling system designed for an open-to-space stator might possibly achieve a low temperature rise of approximately 180°F above coolant entrance temperature, but such a system is very complex and would require

extremely close mechanical tolerances, besides introducing some reliability concern with so many (288 per end) heat transfer contact blocks. Each heat transfer block would have to assure a positive clamping pressure. Close to the rows of such radially locked-in heat transfer blocks, circumferentially arranged liquid metal coolant passages would also be required. In order to simplify such a heat transfer block stator cooling system, the electrical pump design would have to be compromised to fewer turns per coil, which means higher input currents and much lower voltages resulting in an impractical design. The reliability of such heat transfer blocks has not been proven. At the present time their application appears more suitable for space generator designs with a one turn per coil winding arrangement.

Water cooled hollow copper conductors are commercially available, some in standard sizes ranging from outside diameters of 0.144 in. to 0.46 in. In turbogenerators, for example, multi-turn windings with liquid headers have been installed. In the present case of a liquid metal cooling system, hollow silver conductors with stainless steel cladding inside and outside would be required. Since NaK is also a good electrical conductor, it, too, would carry current.

The necessary hydraulic arrangement for the coolant flow and the electrical grounding requirements of such a system add greatly to its mechanical complexity. The feasibility and reliability of this system as applied to this EM pump design is not readily predictable.

Since a very even winding temperature could be achieved, with this system, it might produce the lowest winding hot spot temperature for open-to-space EM pump designs. However, similar to the heat transfer block design, it is better suited to a very small number of turns per coil. The interaction of a moving, electrically conductive liquid in the hollow conductors within the magnetic field has not been evaluated.

None of the three "open-to-space" heat transfer systems as discussed, can be readily applied to a feasible, highly reliable, optimum EM pump design. All three are only in the conceptual design phase and no record of functional reliability has been established.

The gas-filled stators have been built and have established excellent reliability records, besides having adequate heat transfer systems. For this reason, the "gas-filled stator concept" has been chosen as the most reliable and feasible for the final design. The final design is really a combination of the canned pump and canned stator arrangements for the utmost reliability. The entire pump is completely sealed within a rugged frame structure, and in addition, a thin can is inserted into the stator bore to isolate the winding cavity from the immediate duct environment.

B. Design Performance and Characteristics

The operating performance of the pump is calculated through the use of an equivalent circuit as explained in Section V.A, the solution of which has been programmed for a digital computer. This equivalent circuit is shown in Figure 8. Performance curves, shown in Figures 9 through 17, and tabulated values in Tables 1 and 2, show overall calculated performance characteristics for the final designs. Additional calculated results and design characteristics are presented in detail in Tables 3, 4, 5, 6 and 7.

In addition to these results, certain operational limits and conditions are necessary to insure satisfactory operation throughout the pump's life. The principal operational limits are as follows:

1)	Duct and fluid temperature	1300°F maximum
2)	Stator coolant flow rate - NaK	6 gpm minimum
3)	Duct pressure	350 psia maximum
4)	Stator cavity pressure at Room Temperature	6 psia minimum 9 psia maximum
5)	Net positive suction head	See Table 8
6)	Stator coolant inlet temperature - NaK	700°F maximum

The limitation on duct and fluid temperature and pressure is primarily one of strength. The duct was originally designed mechanically to safely withstand pressures up to 300 psi at 1300°F maximum. Due to manufacturing limitations with T-111 alloy, the T-111 ducts actually have somewhat thicker walls than necessary from purely a stress standpoint. Although the maximum recommended pressure is 300 psi, the T-111 ducts are capable of withstanding 350 psi for short periods of time at 1300°F. From an operational standpoint the pump is designed for continuous operation at 1000°F and rated flow and developed pressure. It is capable of short time operation at 1300°F at a maximum developed pressure of 250 psi.

The limitation on stator coolant flow rate and temperature is based on the heat exchanger design and a reasonable limit on winding temperature of 1000°F maximum hot spot and 880°F average. The winding and insulation system is capable of temperatures in excess of these amounts. However, both performance and life will be somewhat affected. All calculations are based on an electrical resistivity of the conductor material at an average temperature of 880°F. Average temperatures above this will cause increased winding resistance and losses and lower efficiency.

The limitation on stator cavity pressure depends on both mechanical and electrical considerations. The maximum pressure of 9 psi at room temperature is a mechanical limitation. At operating temperature the pressure in the winding cavity increases by a factor of almost three. To minimize weight the frame structure has been mechanically designed for maximum internal pressures of about 25 psi. Hence, at room temperature internal winding cavity pressure

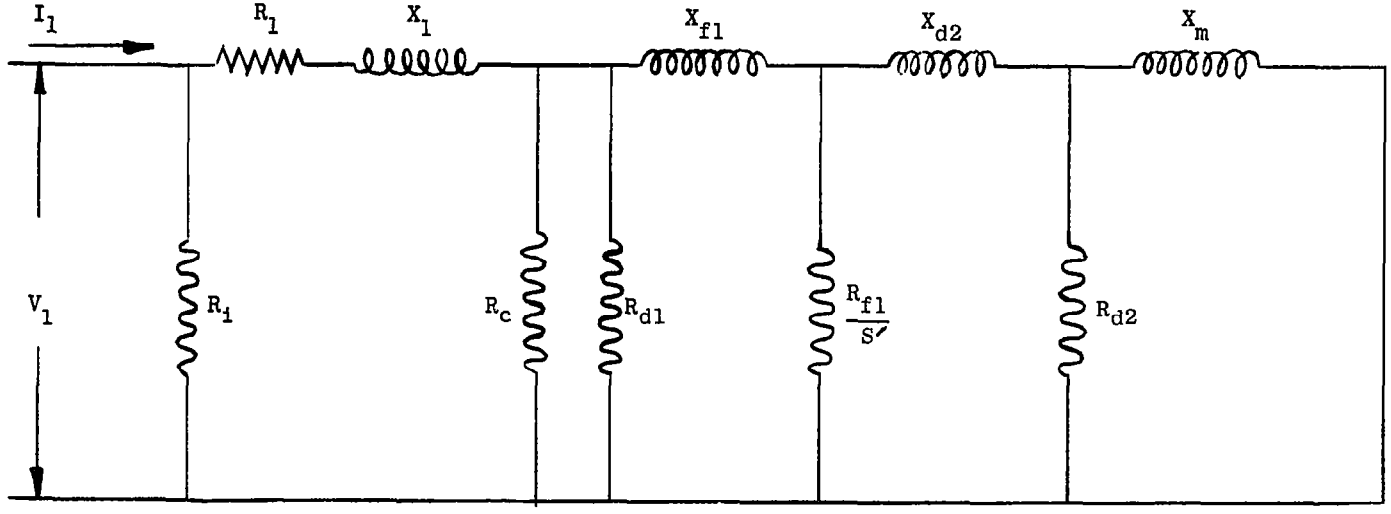

Figure 8. Equivalent Electric Circuit for Helical EM Pump.

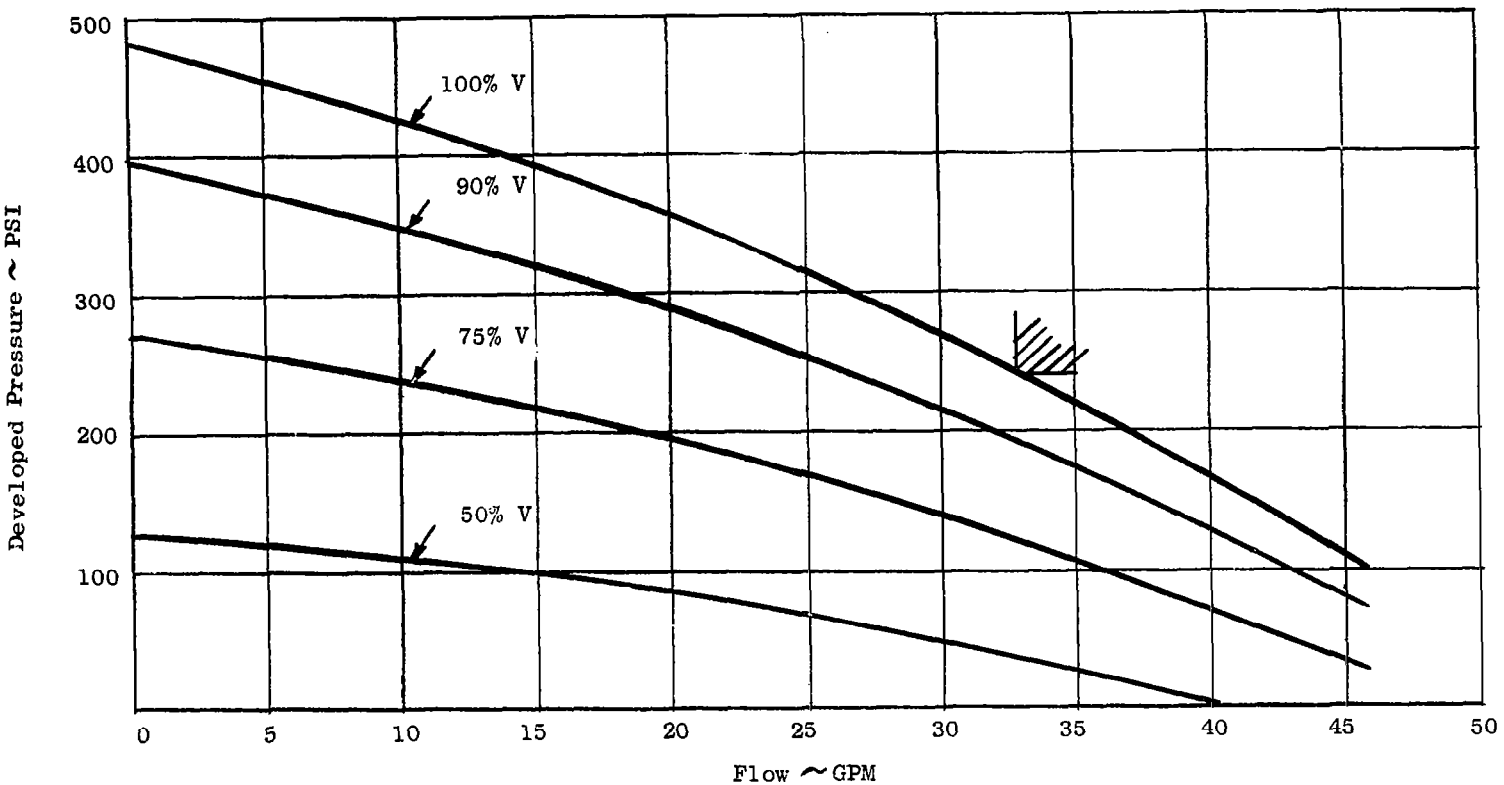

Figure 9. Calculated Performance - Pressure vs Flow EM Pump for Space Power System, Boiler Feed Application. Rating: 32.8 GPM, 240 PSI, 1000°F, Potassium. T-111 Duct.

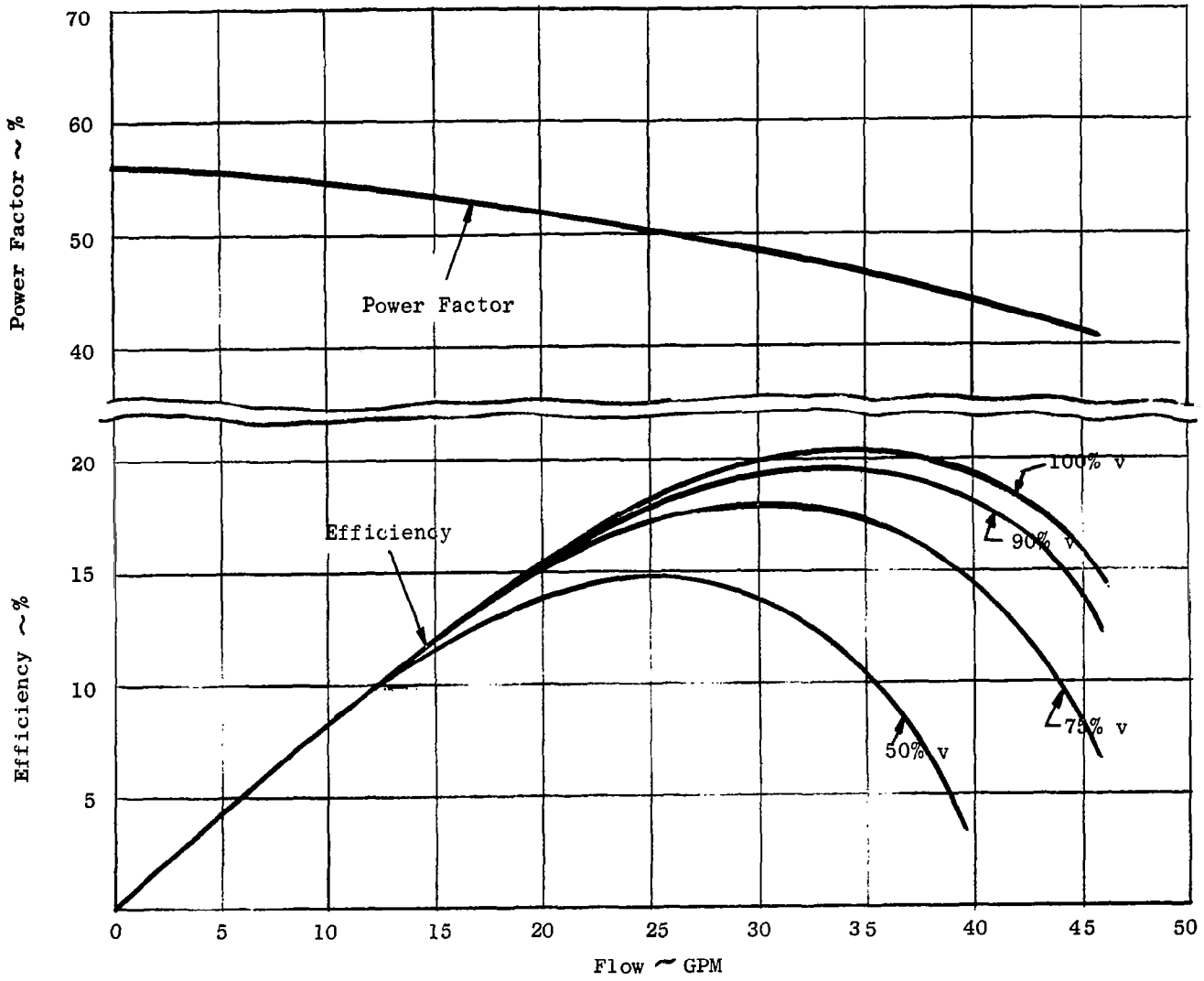

Figure 10. Calculated Performance - Efficiency and Power Factor vs Flow EM Pump for Space Power System Boiler Feed Application. Rating: 32.8 GPM, 240 PSI, 1000°F, Potassium T-111 Duct.

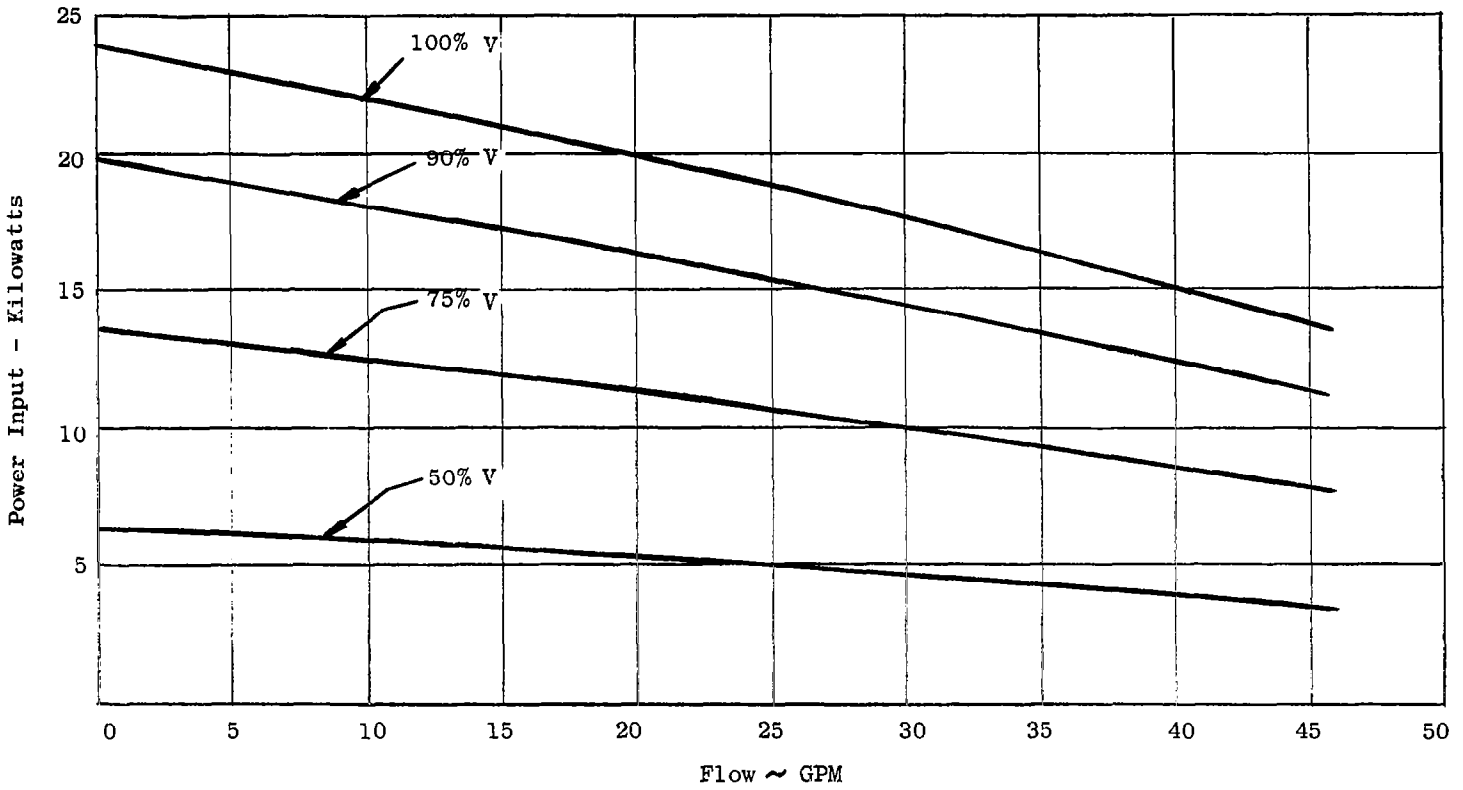

Figure 11. Calculated Performance - Power Input vs Flow EM Pump for Space Power System, Boiler Feed Application. Rating: 32.8 GPM, 240 PSI, 1000°F, Potassium T-111 Duct.

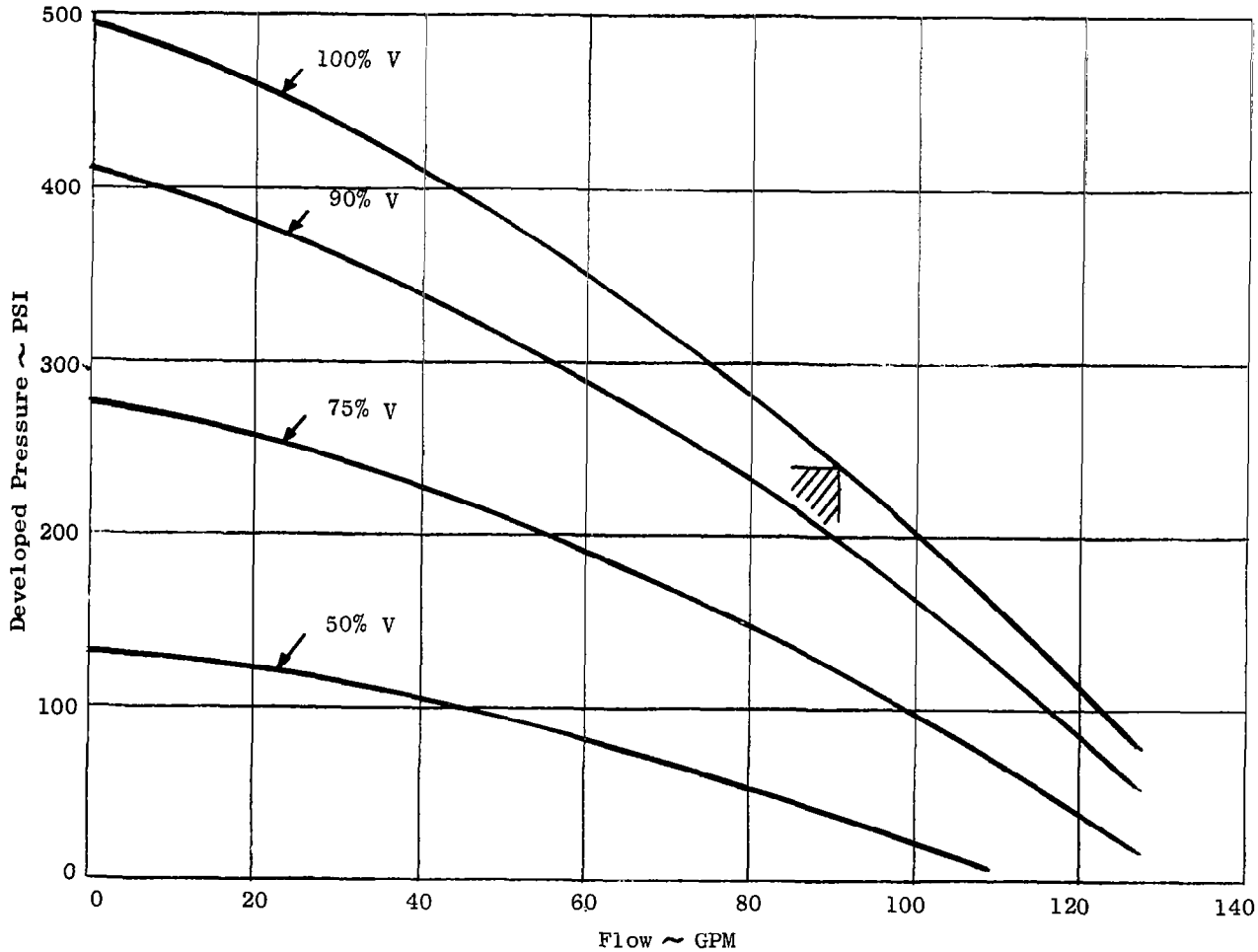

Figure 12. Calculated Performance - Pressure vs Flow EM Pump for Space Power System, Boiler Feed Application. Rating: 90.7 GPM, 240 PSI, 1000°F Potassium. T-111 Duct.

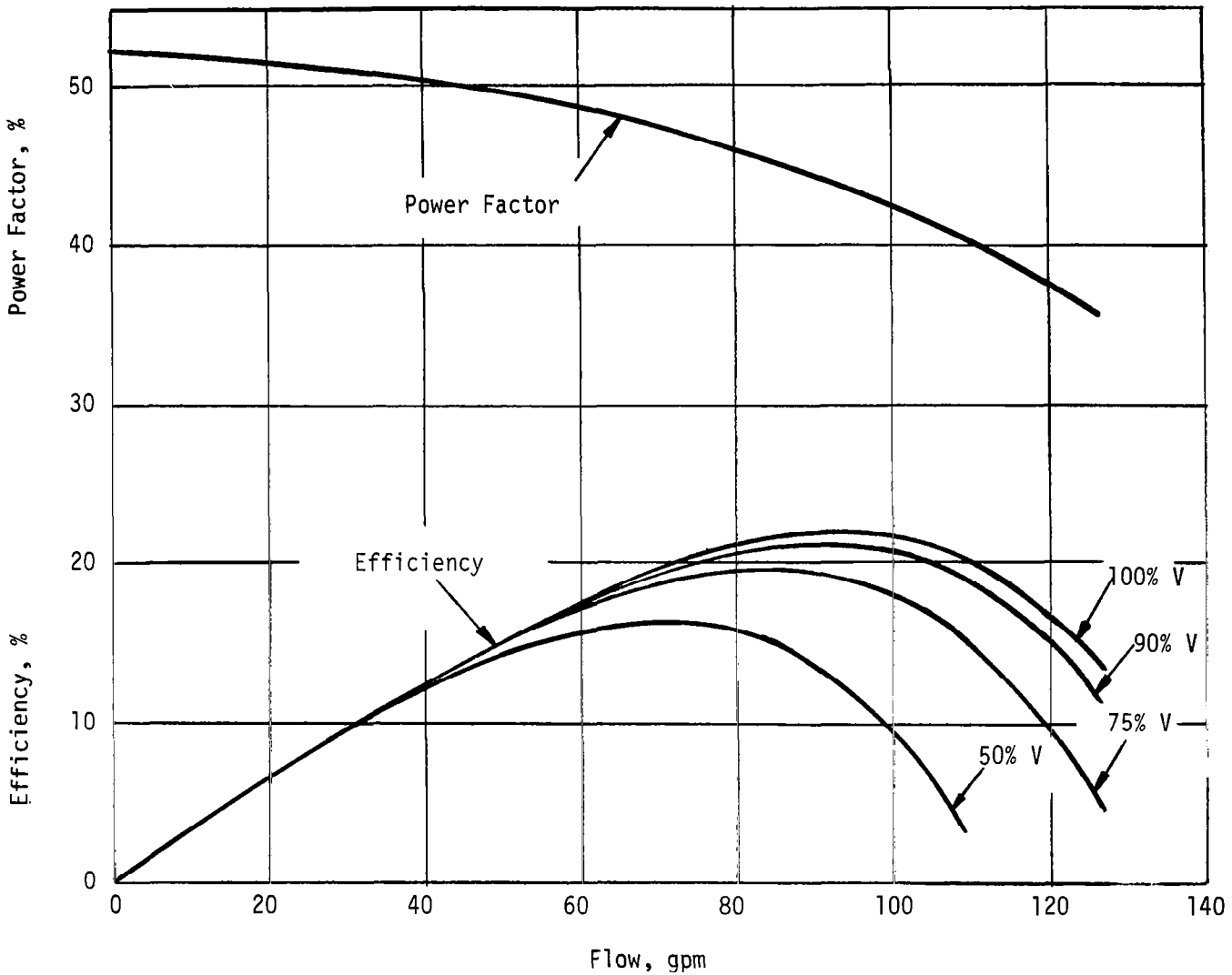

Figure 13. Calculated Performance - Efficiency and Power Factor Vs. Flow (T-111 Duct).

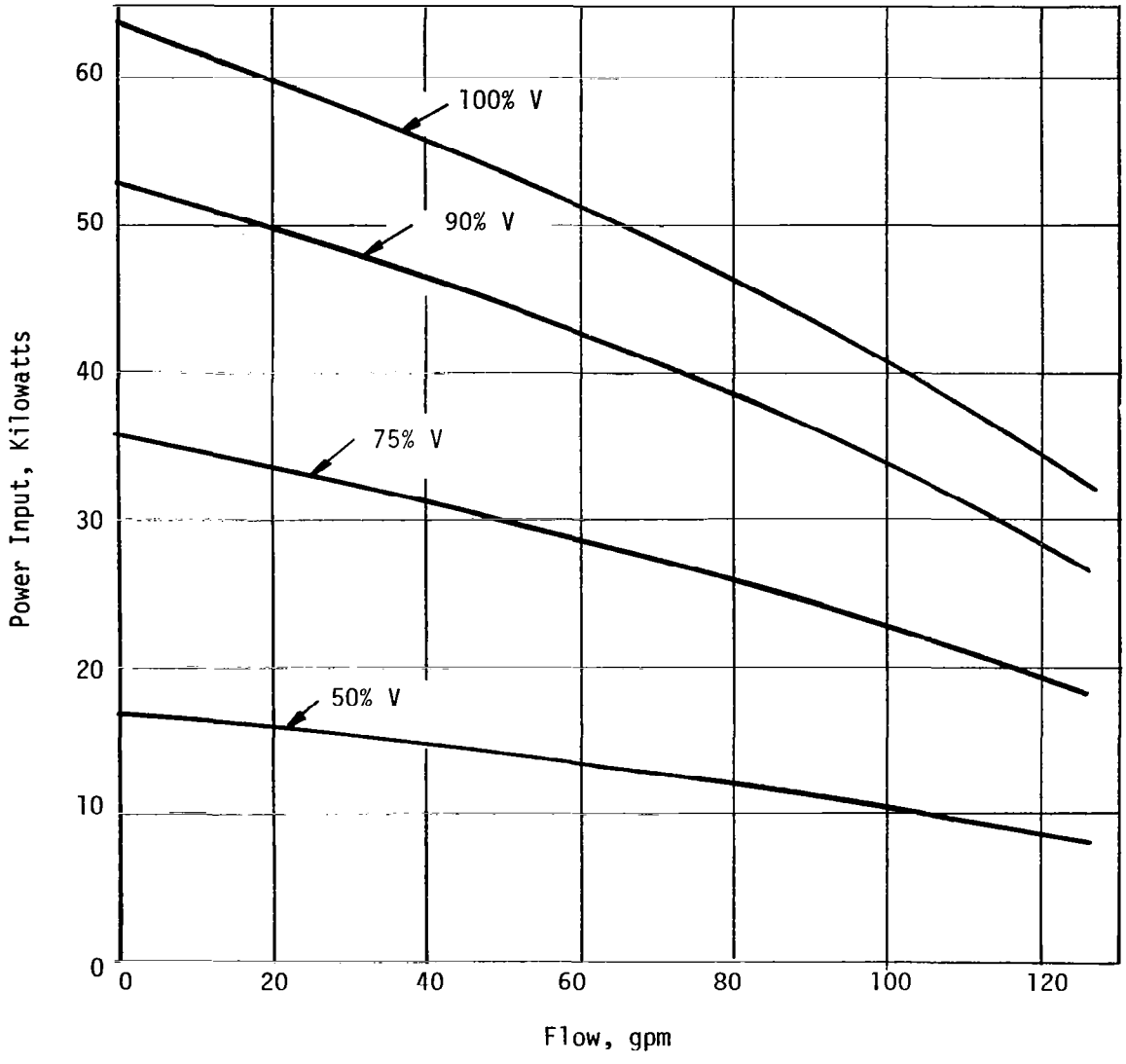

Figure 14. Calculated Performance - Power Input Vs. Flow (T-111 Duct).

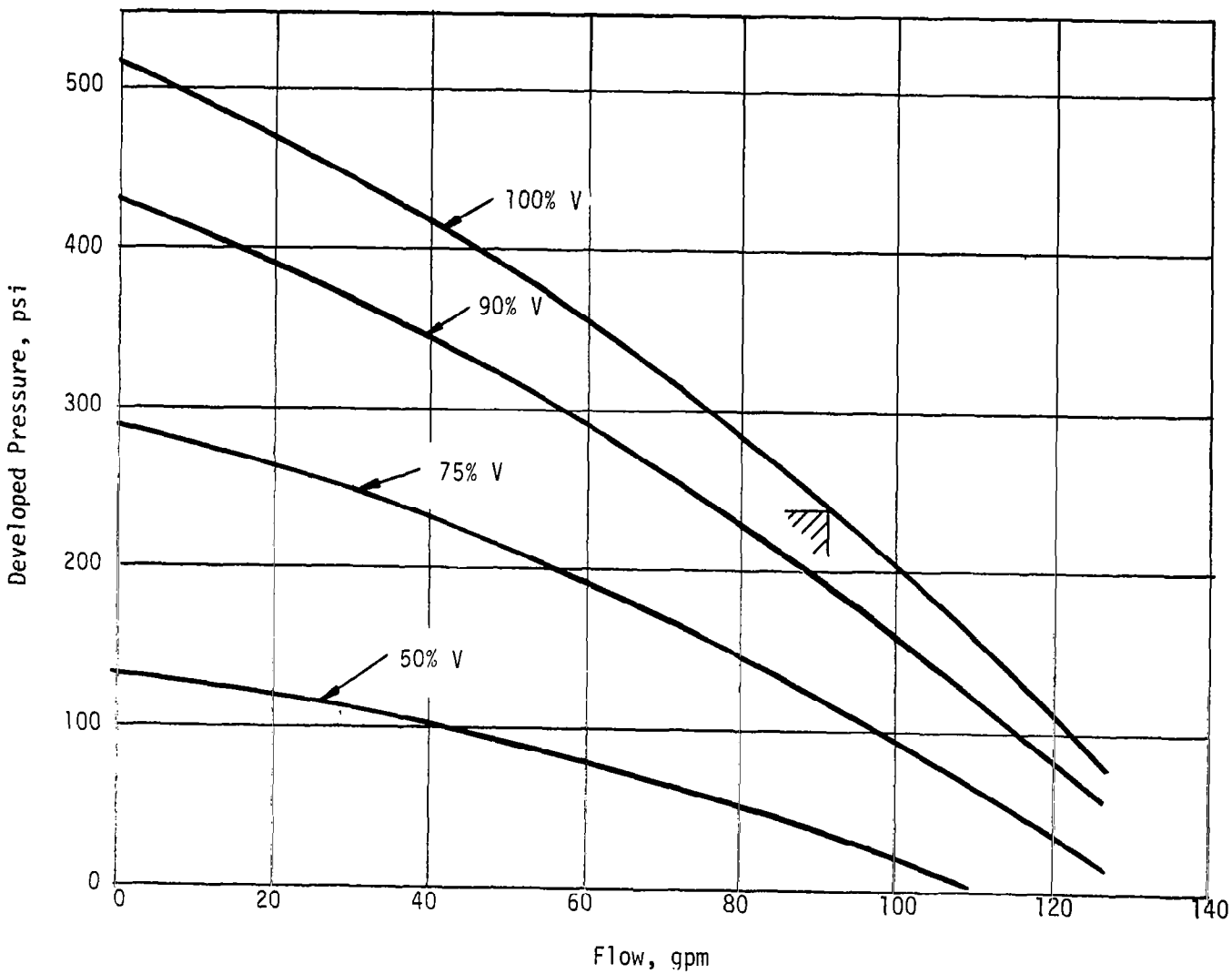

Figure 15. Calculated Performance - Pressure Vs. Flow (316 SS Duct).

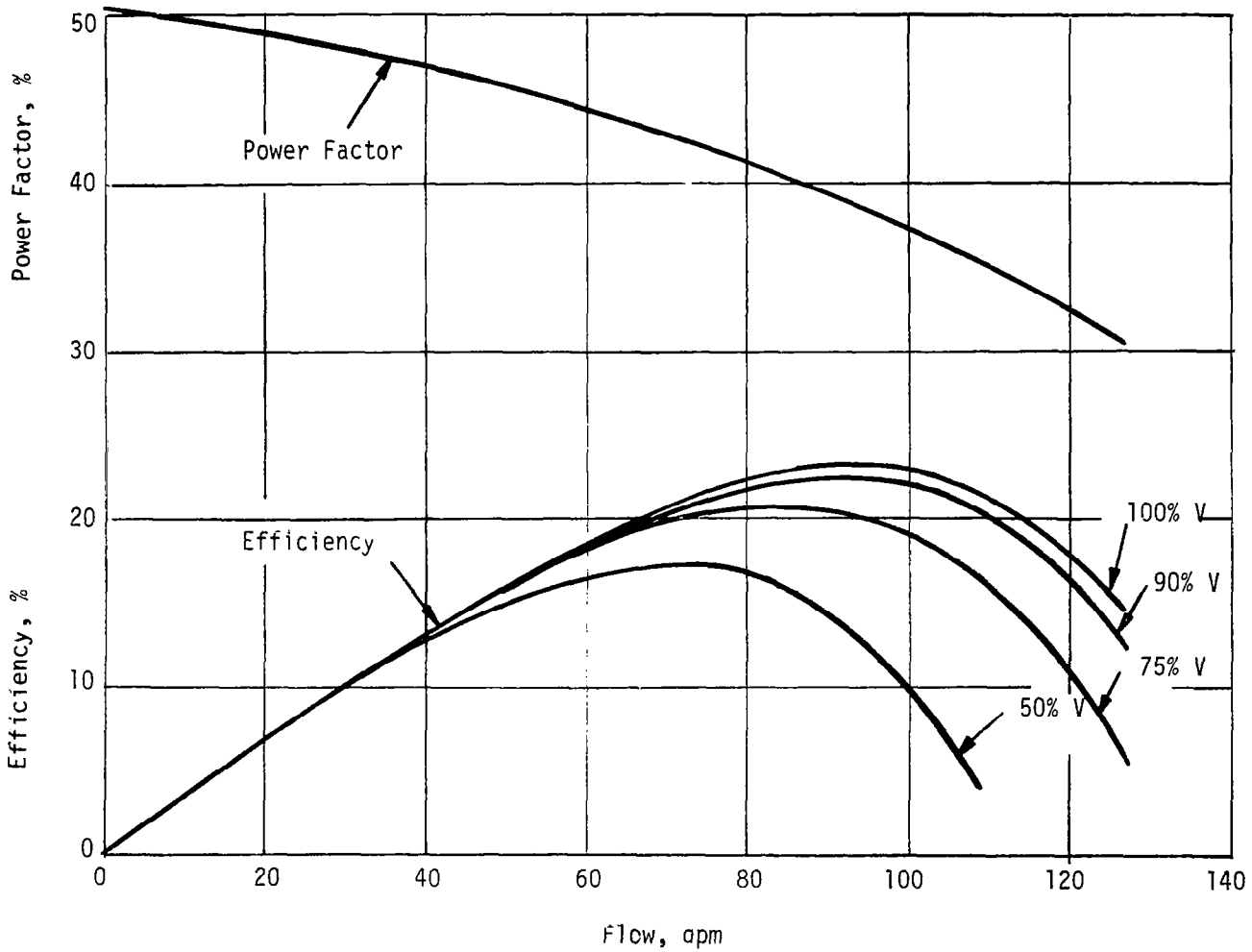

Figure 16. Calculated Performance - Efficiency and Power Factor Vs. Flow (316 SS Duct).

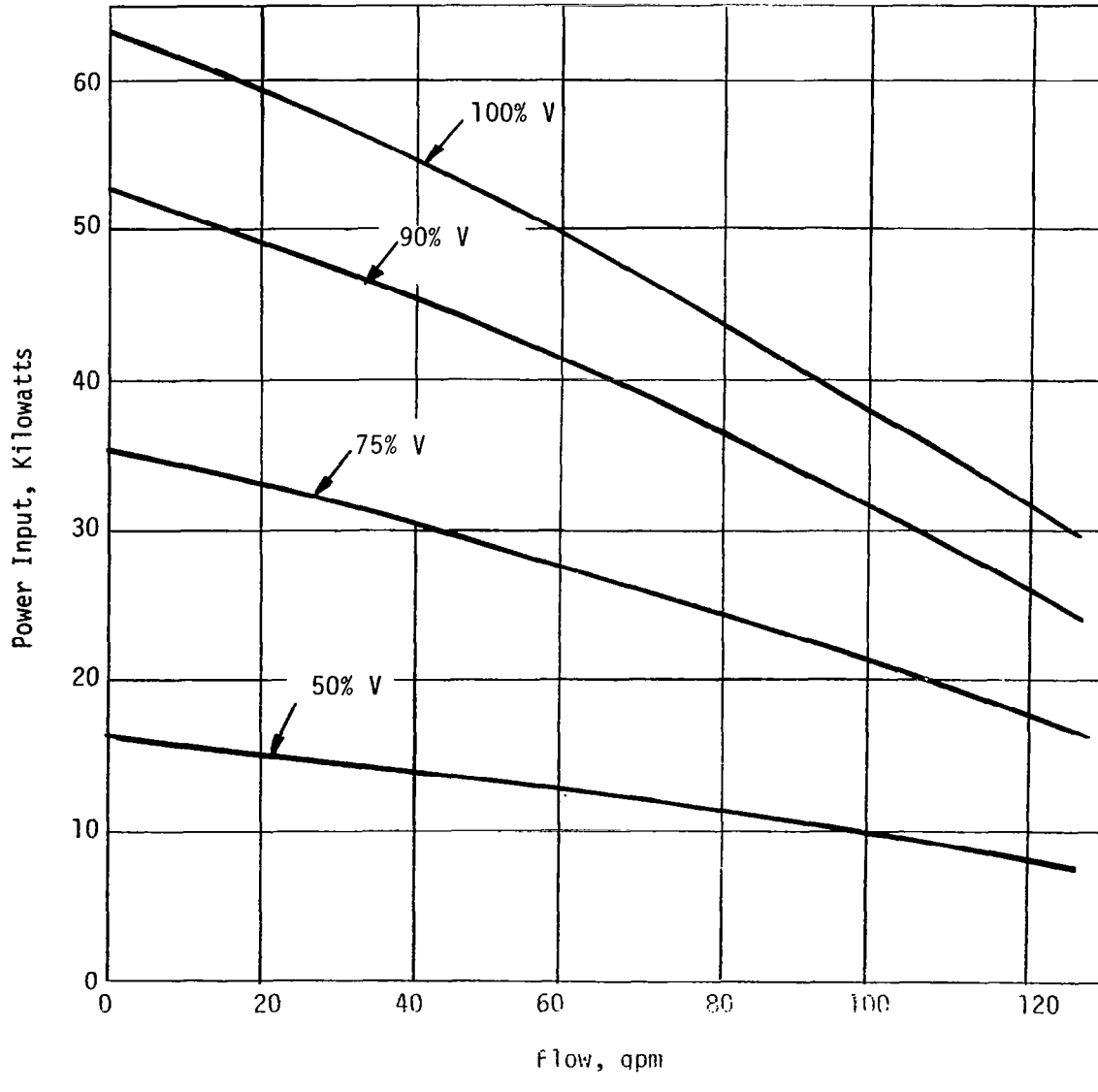

Figure 17. Calculated Performance - Power Input Vs. Flow (316 SS Duct).

TABLE 1. CALCULATED PERFORMANCE CHARACTERISTICS HELICAL INDUCTION EM PUMP (3.25 lb/sec Design)

	T-111 Duct
Fluid	Potassium
Fluid Temperature (°F)	1000
Flow Rate (GPM)	32.8
Developed Pressure (PSI)	240
Power Output (KW)	3.42
Power Input (KW)	17
Efficiency (%)	20
Input (KVA)	36
Power Factor (%)	47
Weight (lbs.)	382
Winding Temperature Rise - Hot Spot (°F)	275
Winding Temperature Rise - Average (°F)	170
Heat Exchanger Requirements	
- Flow (GPM)	6
- Pressure Drop (PSI)	9
- Total Heat Load (KW)	6
- Coolant Inlet Temperature (°F)	650

TABLE 2. CALCULATED PERFORMANCE CHARACTERISTICS HELICAL INDUCTION EM PUMP
(9 lb/sec Design)

	T-111 Duct	316 Stainless Steel Duct
Fluid	Potassium	Potassium
Fluid Temperature (°F)	1000	1000
Flow Rate (GPM)	90.7	90.7
Developed Pressure (PSI)	240	240
Power Output (KW)	9.47	9.47
Power Input (KW)	43	40
Efficiency (%)	22	23.5
Input (KVA)	98	102
Power Factor (%)	44	39
Weight (lbs.)	775	745
Winding Temperature Rise - Hot Spot (°F)	300	300
Winding Temperature Rise - Average (°F)	165	165
Heat Exchanger Requirements		
- Flow (GPM)	8	8
- Pressure Drop (PSI)	16	16
- Total Heat Load (KW)	10	10
- Coolant Inlet Temperature (°F)	650	650

TABLE 3. DETAILED ELECTRICAL DESIGN CHARACTERISTICS
CALCULATED VALUES AT DESIGN POINT

	3.25 lb/sec (T-111 Duct)	9 lb/sec (T-111 Duct)	9 lb/sec (316 SS Duct)
Efficiency (%)	20	22	23.5
Power Factor (%)	47	44	39
Line Current (amps)	145	350	350
Line Voltage (volts)	145	160	170
Losses and Power Requirements			
-Stator Winding I^2R (KW)	3.85	7.1	7.1
-Iron Loss (KW)	1.0	2.2	2.2
-Stator Can Loss (KW)	0.3	0.7	0.8
-Duct Loss (KW)	3.62	10.0	7.0
-Hydraulic Loss (KW)	0.52	1.5	1.4
-Fluid (Slip) Loss (KW)	4.23	12.0	12.0
-Total Losses (KW)	13.6	33.5	30.5
-Output (KW)	3.42	9.47	9.47
-Input (KW)	17.0	43	40
-Input (KVA)	36	98	102
Slip	0.44	0.42	0.42
Winding Current Density (amps/in^2)	2550	2800	2800
Tooth Peak Flux Density (k lines/in^2)	48	48	52
Yoke Peak Flux Density (k lines/in^2)	70	65	68
Center Iron Peak Flux Density (k lines/in^2)	79	85	98
Gap Peak Flux Density (k lines/in^2)	14	14	15

TABLE 4. DETAILED HYDRAULIC DESIGN CHARACTERISTICS
CALCULATED VALUES AT DESIGN POINT

	3.25 lb/sec (T-111 Duct)	9 lb/sec (T-111 Duct)	9 lb/sec (316 SS Duct)
Velocity of Fluid in Duct (ft/sec)			
- First turn of helix	20.2	20.5	20.6
- Second turn of helix (average)	25.7	28.2	28.2
- Remaining turns of helix	31.1	35.8	35.9
Velocity Head of Fluid in Ducts (psi)			
- First turn of helix	1.96	2.02	2.04
- Second turn of helix (average)	3.18	3.82	3.82
- Remaining turns of helix	4.65	6.15	6.19
Total Hydraulic Loss thru Duct (psi)	36.5	33.9	32.1

TABLE 5. DETAILED THERMAL DESIGN CHARACTERISTICS
CALCULATED VALUES AT DESIGN POINT

	3.25 lb/sec (T-111 Duct)	9 lb/sec (T-111 Duct)	9 lb/sec (316 SS Duct)
Winding Hot Spot Temperature Rise (°F)	275	300	300
Winding Average Temperature Rise (°F)	170	165	165
Heat Load from Duct through Thermal Insulation (KW)	0.59	1.12	1.12
Total Heat Load to Coolant (KW)	6	10	10
Coolant (NaK) Flow Required (GPM)	6	8	8
Coolant (NaK) Inlet Temperature (°F)	650	650	650
Coolant (NaK) T mperature Rise (°F)	50	50	50
Coolant (NaK) Pressure Diop (PSI)	9	16	16
Heat Generated in Duct and Fluid (KW)	8.4	20.5	18.1
Fluid (Potassium) Temperature Rise (°F)	12.5	11.3	9.9

TABLE 6. DETAILED MECHANICAL DESIGN CHARACTERISTICS
CALCULATED VALUES (PSI) DUE TO PRESSURE LOADING

	3.25 lb/sec (T-111 Duct)	9 lb/sec (T-111 Duct)
Frame Structure		
- Design Pressure	25	25
- Maximum Primary Hoop Stress in Frame	1,062	1,200
- Maximum Stress in End Shield - Conn. End	19,375	19,740
- Maximum Stress in End Shield - Opp. Conn. End	12,100	12,860
- Maximum Bending Stress in Frame	13,530	10,500
Duct		
- Design Pressure	350	300
- Maximum Primary Hoop Stress in Duct	29,000	26,700
- Maximum Stress in End Cap	7,060	7,300
- Maximum Bending Stress in Duct (primary and secondary)	31,400	26,700

TABLE 7. DETAILED WEIGHT CHARACTERISTICS (POUNDS)
CALCULATED VALUES

	3.25 lb/sec	9 lb/sec	
	(T-111 Duct)	(T-111 Duct)	(316 SS Duct)
Stator			
- Magnetic Core	131	306	
- Winding	99	215	
- Frame and Heat Exchanger	67	139	
- Miscellaneous	22	32	
Duct			
- Helical Duct and Wrapper	20.5	28	18
- Center Magnetic Core	10.5	16	16
- Inlet/Outlet Connector	23	27	13
- Miscellaneous	9	12	6
Total Weight	382	775	745

TABLE 8. NPSH REQUIREMENTS

NPSH (psi)	Maximum Recommended Flow	
	3.25 lb/sec Design	9 lb/sec Design
3	2.8 lb/sec	7.8 lb/sec
4	3.25 lb/sec	9 lb/sec
5	3.6 lb/sec	10 lb/sec
6	3.95 lb/sec	11 lb/sec
7	4.25 lb/sec	12 lb/sec

must be limited to about 9 psi. It is unreasonable to add weight to the frame to design it for unnecessarily high pressures. The lower limit of 6 psia is based on electrical reasons. Because of reduced arc-over voltage of the winding and insulation system at pressures below about 6 psi, it is recommended that this be the minimum winding cavity pressure at room temperature. This gives a pressure of just slightly greater than atmospheric at operating temperature.

The limitation on net positive suction head is based on cavitation considerations, using the criterion of requiring an NPSH of at least two velocity heads at entrance to the pumping section. This criterion is explored in Reference 1 and appears to be reasonably conservative. Flow rates for several values of NPSH for each design are based on this criterion.

At the design point of 1000°F, 240 psi developed pressure, 7 psi NPSH and rated flow (3.25 lb/sec or 9 lb/sec) the pump can operate continuously. At 1000°F or less it can operate continuously over a range of flow rates from 45% to 130% rated flow rate, at developed pressures up to 240 psi, as long as the NPSH requirements in Table 8 are compiled with.

The pump can operate for periods of time at 1000°F at developed pressures up to 250 psi over the same flow rate range as above. At 1300°F the pump can also operate for periods of time over the same range of flow rates and up to 250 psi developed pressure. Of course, the performance will not be as good as at the design point. The principal limitation on time of operation is winding temperature and duct temperature. These temperatures should not be allowed to exceed the recommended limits. By appropriate increases in NaK coolant flow rate or decreases in NaK coolant temperature it may be possible to operate continuously at some of these other points.

C. Discussion of Significant Parameters

There are several significant parameters which were varied in this analytical study to determine the final design which represents a balance of optimum efficiency, maximum reliability, minimum weight and production feasibility. The most important parameters once a set of materials and the basic concept have been selected, are (1) fluid passage cross-sectional geometry (2) duct wall thicknesses and total magnetic gap (3) frequency (4) duct, fluid passage and stator diameters (5) duct and stator length and (6) velocity and slip as determined by the interrelation among frequency, fluid passage geometry and diameter. All of these parameters were varied over a considerable range in this design study. Several hundred computer runs were made to cover a multitude of combinations of these variables.

Fundamentally a helical induction EM pump is a relatively low flux density machine due to its large magnetic (air) gap compared to conventional induction motors. Large magnetizing currents become necessary to establish the required flux levels in the gap which in turn result in relatively lower power factors. Hence, it is desirable to make the gap between the stator core and center iron structure as small as possible by keeping the thermal insulation thin, the duct

walls thin and the fluid passage height small. Thin duct walls are also desirable to reduce I^2R losses in the duct since these are directly proportional to duct thickness.

Fluid velocity and slip are very important parameters and are established by the fluid passage geometry, frequency and diameters. Various combinations of these parameters must be investigated to determine optimum values.

In a study such as this to determine the best design which meets certain specification requirements, it becomes quite clear very early in the design phase that no sharp optimum exists. Because of the interrelation among so many variables, there are several designs which meet the requirements, any one of which could be considered optimum by certain individuals. Hence, selection of the final design involves a considerable amount of judgment and experience.

For example, the optimum frequency for these designs occurs over a range of about 45 - 70 cps. Frequencies below 45 cps require considerably larger diameters for good performance, and hence result in a much heavier unit. Frequencies above 70 cps require such small diameters that it becomes impossible to build besides resulting in poorer performance.

From about 50 - 65 cps the duct and stator diameters and flow passage geometry can be selected such that performance is basically a standoff.

Based on this, a final frequency of 60 cps was selected as the most practical value since this permits a unit to be very easily tested once it is built. A special frequency power supply would not be required for testing.

It is desirable to operate induction EM pumps at relatively high velocities and low slip for efficient operation. However, velocity is limited by hydraulic loss and NPSH. In addition as the slip decreases the efficiency at the design point eventually goes through a maximum, since fluid (slip) loss decreases while winding and duct I^2R loss increases with decreasing slip.

Current density, another important design characteristic, since it directly affects winding temperature, goes through a minimum as the slip is decreased due to the load component of current decreasing while the magnetizing component is increasing. It is desirable to select a velocity, slip and corresponding flow passage geometry (cross-section and diameter) to give peak efficiency and minimum winding current density at the design point. Since these do not occur at precisely the same point the final design must provide the proper balance between efficiency and current density factoring in hydraulic loss and NPSH.

The conflict between low NPSH and high velocity in the duct is resolved in these designs by employing a dual pitch helical duct. The first two turns of the machined helical duct have a relatively large pitch to maintain low velocity near the pump entrance where the NPSH is low. Then as pressure is developed in the pump the pitch of the helix is reduced for the remaining turns to give a higher fluid velocity and more efficient pumping.

D. Power Conditioning Requirements

The final EM pump designs require a three phase 60 cps power supply for proper operation. Calculated voltage, current and power requirements are shown in Table 9 for each design.

Typical power systems that might be available in a Rankine cycle space electric power system for the EM pump power supply are:

1) 400 cps - 3 phase - 1000 volts, rms., line-to-neutral

2) 1200 cps - 3 phase - 1000 volts, rms., line-to-neutral

There are several means by which the desired voltage and frequency can be obtained from these power sources. Dynamic conversion (motor-generator set) is undesirable because of the inherent heavy weight of low frequency machinery, and the fretting and wear problems of materials. Also, the output frequency of the motor-generator set can not be adjusted. The most common static conversion method, rectification followed by inversion, has also severe disadvantages; namely, it requires large commutational capacitors and heavy low frequency transformers.

For power conditioning equipment for the EM pump, a "Synchronous Static Frequency Divider" with a high frequency transformer is recommended. The "Synchronous Static Frequency Divider" reduces the generator frequency to the frequency range suitable for the pump. A transformer is used to reduce the generator output voltage to the voltage level required by the pump. The following sections on power conditioning requirements briefly describes the frequency divider, the input transformer, and the control of the pump. The numerical values given in these sections refer to the 3.25 lb/sec pump. All the numerical results are tabulated in Tables 12 and 13 for the 9 lb/sec pump.

1. The Synchronous Static Frequency Divider

The basic block diagram of a Static Frequency Divider is shown in Figure 18. The function of the logic circuitry is to provide the control signal for the SCRs in the proper time and sequence.

a. Silicon Controlled Rectifier Circuit. The section of this device incorporating the silicon controlled rectifiers, shown in detail in Figure 19, is the circuit which handles the power and produces the low frequency output voltages. These low frequency output voltages are obtained by alternately providing a series of positive dc voltages and then a series of negative dc voltages from the high frequency three phase input to each phase of the output.

b. Pulse Generating Circuits. The rectifier pulse generating circuit and the inverter pulse generating circuit are the first elements in the generation of the control signals for the SCRs. Rectifier pulses are used for commutation within a group of SCRs. The inverter pulses are used for two purposes; to promote commutation between the positive and the negative groups of SCRs when the load is inductive, and also to drive the counter circuit.

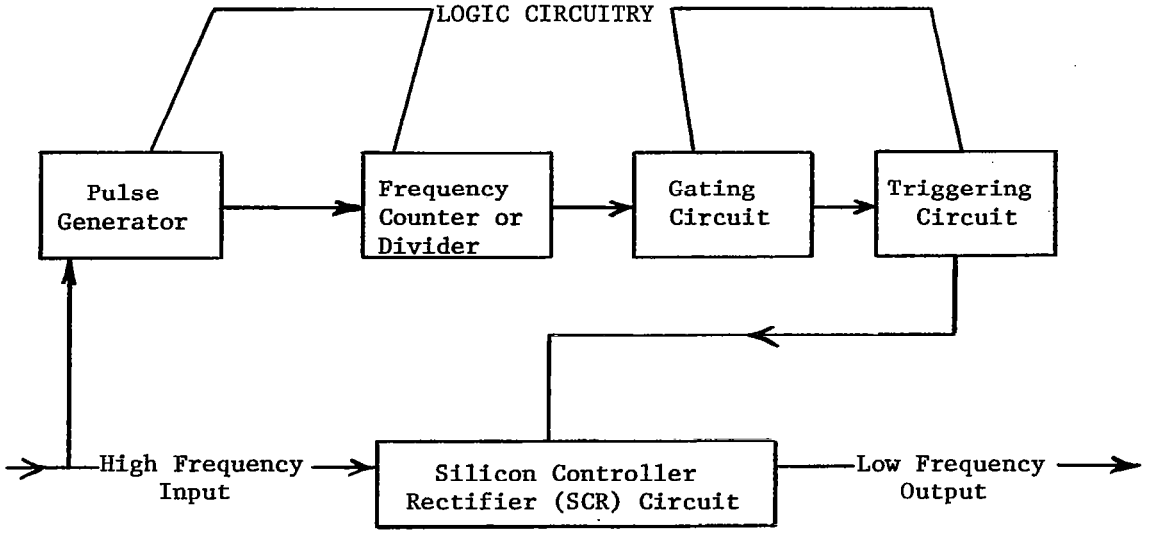

Figure 18. Block Diagram Static Frequency Divider.

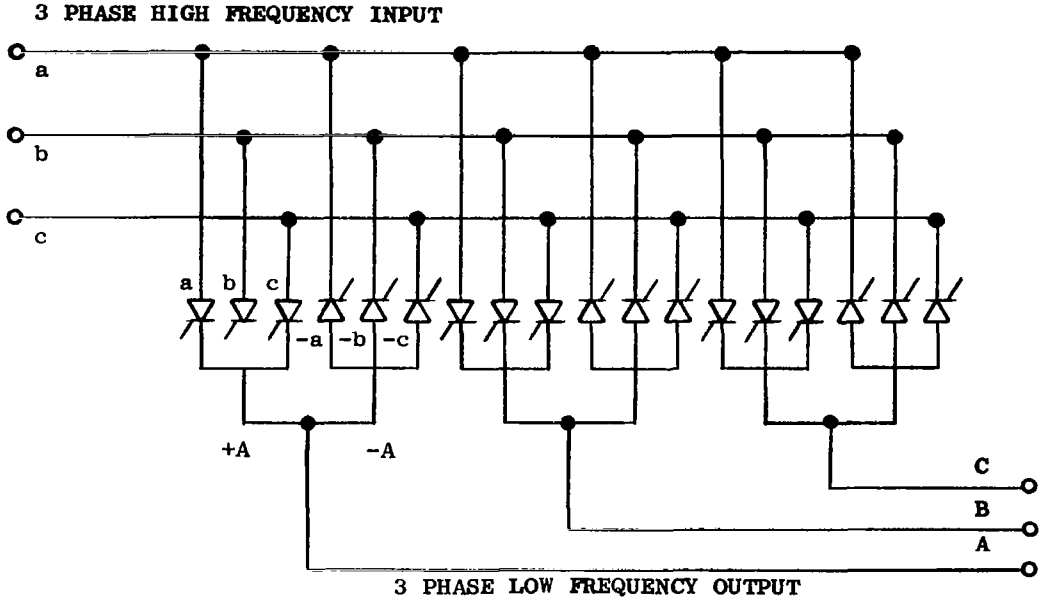

Figure 19. Synchronous Static Frequency Divider.

TABLE 9. POWER SUPPLY REQUIREMENTS

	3.25 lb/sec Design (T-111 Duct)	9 lb/sec Design (T-111 Duct)	9 lb/sec Design (316 SS Duct)
Design Point Flow Rate			
- 20 psi, 1000°F			
V_L	145	160	170
I_L	145	350	350
KW_{in}	17	43	40
KVA_{in}	36	98	102
- 240 psi, 1300°F			
V_L	170	195	205
I_L	165	355	360
KW_{in}	20	45	41
KVA_{in}	48	120	130
130% Design Point Flow Rate			
- 250 psi, 1000°F			
V_L	185	220	230
I_L	175	400	400
KW_{in}	23	55	50
KVA_{in}	55	150	160
- 250 psi, 1300°F			
V_L	220	280	300
I_L	205	485	500
KW_{in}	28	75	65
KVA_{in}	80	240	260

Table 10. Summary of Equipment Characteristics for 400 cps Input Frequency. (3.25 lb/sec)

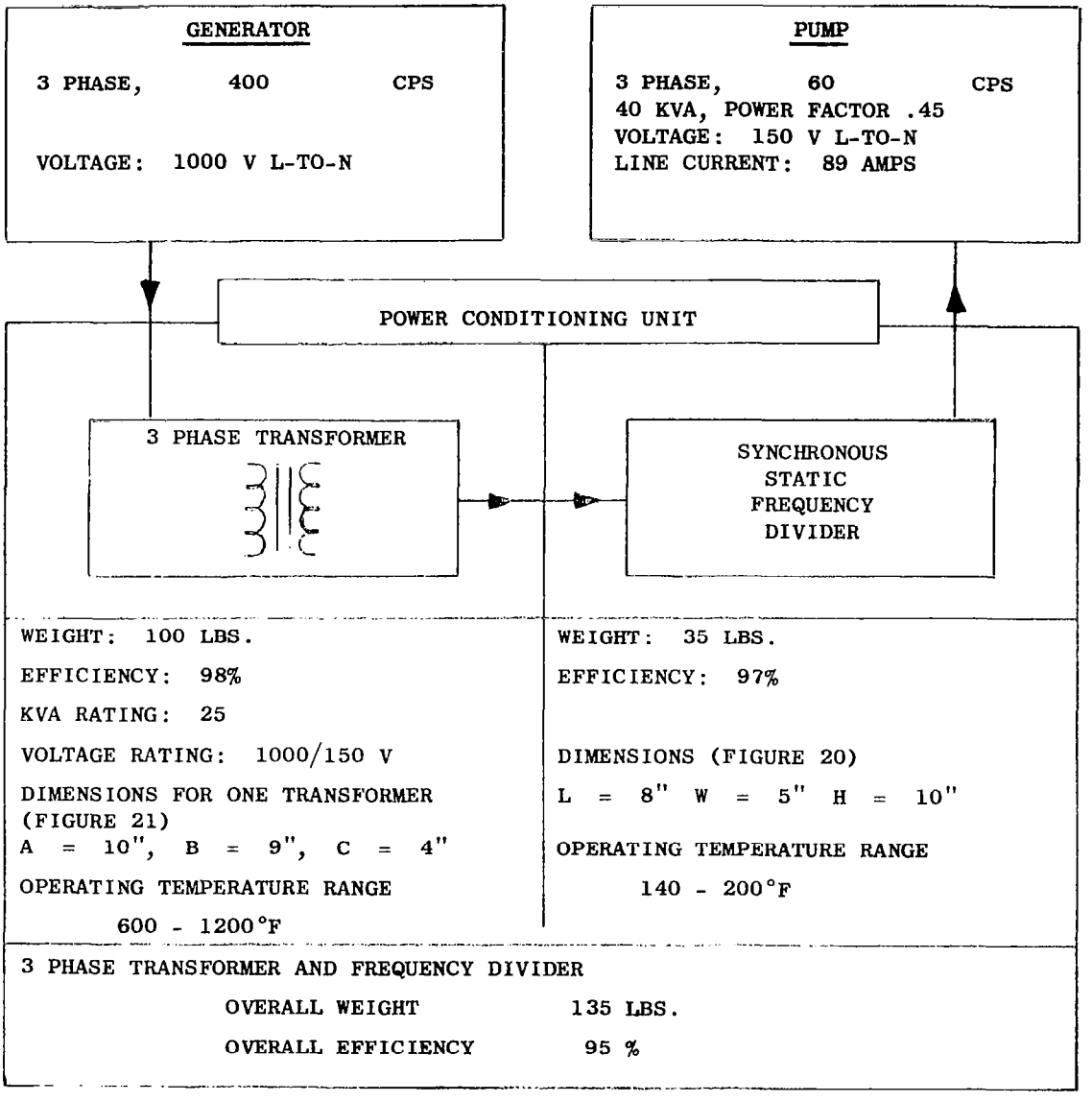

Table 11. Summary of Equipment Characteristics for 1200 cps Input Frequency. (3.25 lb/sec)

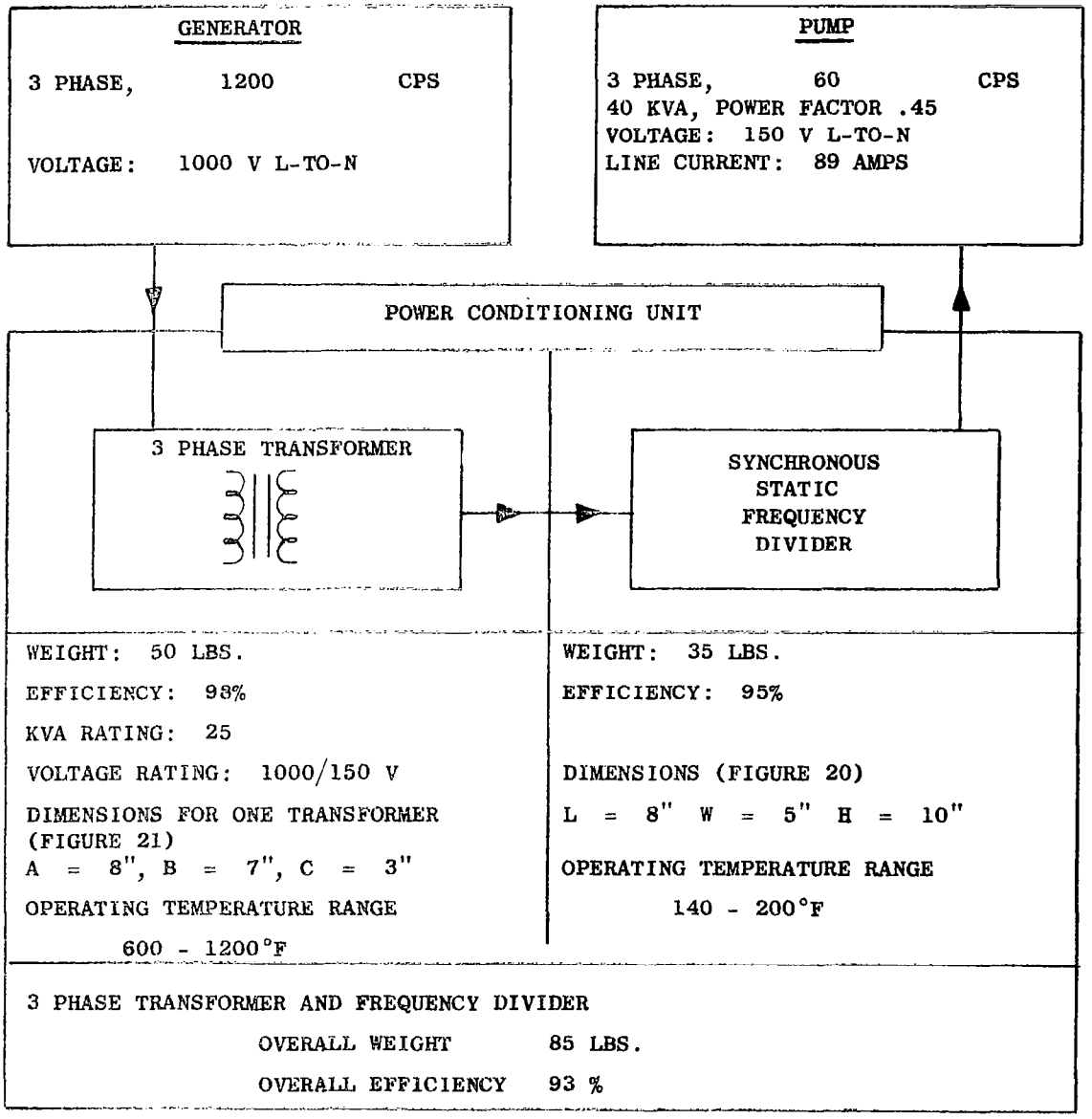

Table 12. Summary of Equipment Characteristics for 400 cps Input Frequency. (9 lb/sec)

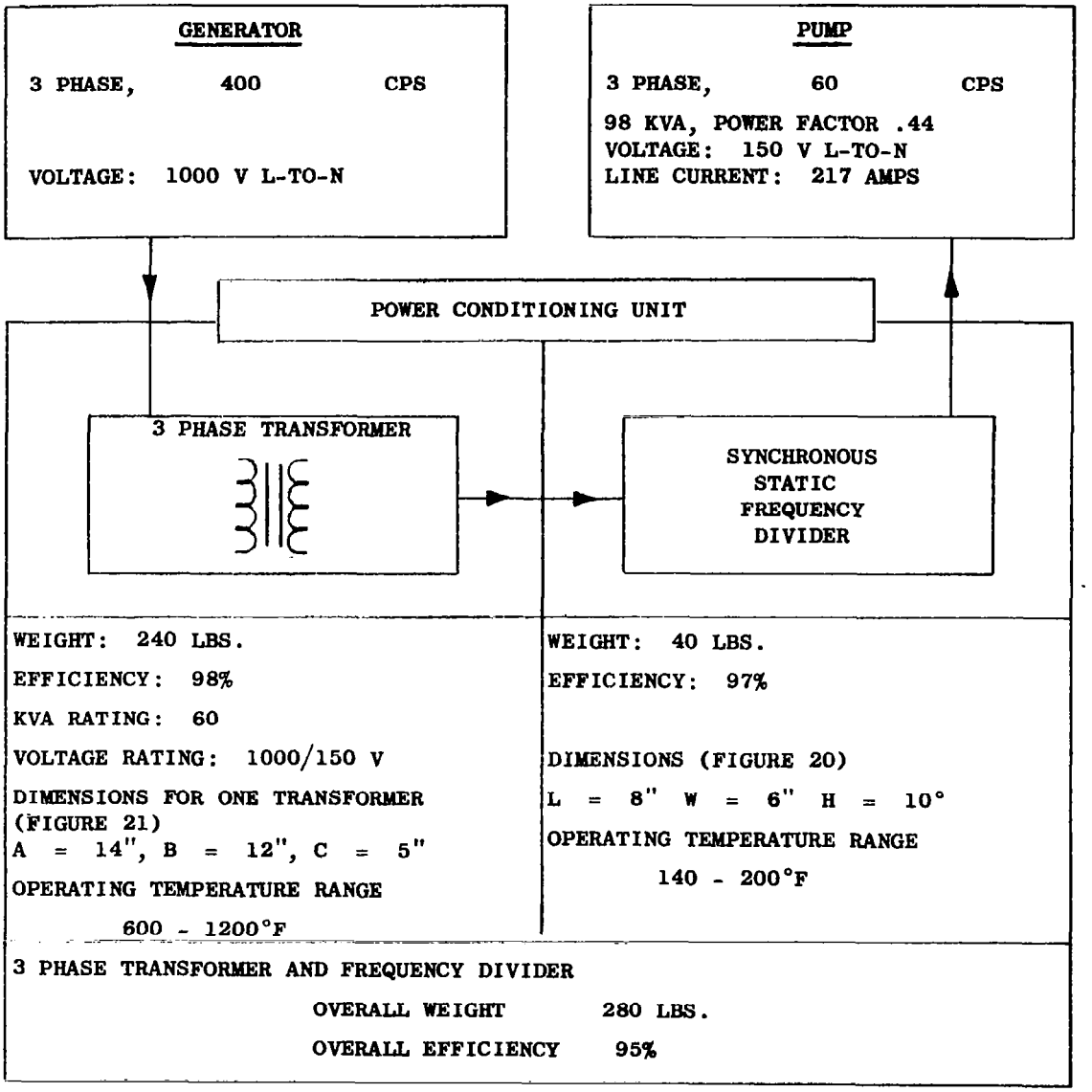

Table 13. Summary of Equipment Characteristics for 1200 cps Input Frequency. (9 lb/sec)

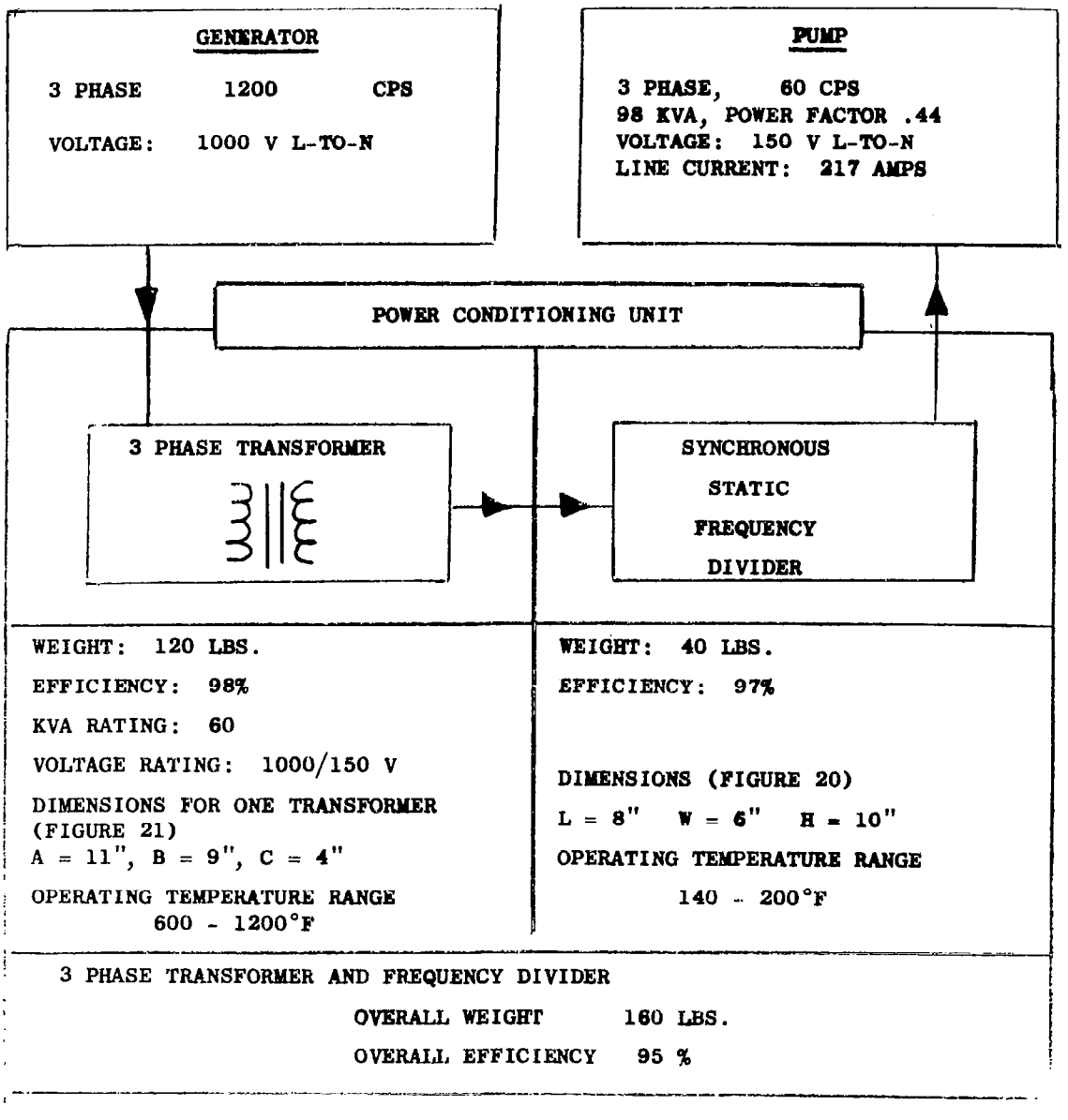

c. Frequency Counter or Divider. The purpose of the counter circuit is to generate the on and off pulses, in the desired time sequency to control the gating circuit. This counter circuit is a binary coded counter which divides the input by the desired frequency ratio.

d. Gating Circuit. The function of the gating circuit is to provide the proper sequency for turning the SCRs on and off by either permitting or suppressing the rectifier pulses.

e. Triggering Circuit. The function of the triggering circuit is to provide the triggering signals to the gate of the SCRs. This circuit combines and amplifies the gating signals, the rectifier pulses, and the inverter pulses.

An isometric view of the proposed frequency divider is shown in Figure 20. This is a complete unit showing the eighteen SCRs and their mountings, the wiring for the SCRs, the logic circuitry, and the box type structure with provision made for cooling. The power input and output terminals are also indicated on the figure. For a 40 KVA pump, the approximate size of the frequency divider is length (L) 8 inches, width (W) 5 inches, and height (H) 10 inches. The approximate weight of the unshielded frequency divider is 35 pounds for either 400 cps or 1200 cps input frequency.

2. Input Transformer

Since the 1000 volt line to neutral voltage is too high to be used to drive the EM pump, the power conditioning equipment involves a transformer to reduce the voltage level to that required by the pump.

With the use of the Synchronous Static Frequency Divider the transformer need not be rated to the full load KVA, because of the inherent power factor correcting capability of the Synchronous Static Frequency Divider. This correction is due to the fact that the energy stored in the magnetic field of the load is constantly being shifted by the frequency converter from one low frequency phase to another without going back to the transformer. For a conservative design the transformer should be rated for a 0.80 power factor. The 3.25 lb/sec pump requires about 18 KW; the corresponding value of KVA at 0.80 power factor is 22.5 KVA. The transformer is sized for 25 KVA to accommodate the losses involved with the Synchronous Static Frequency Divider.

1) At 400 cps the weight of a 25 KVA open construction transformer is estimated to be 100 lb. at 98% efficiency.

2) For the same ratings, but for 1200 cps, the estimated weight for the transformer is 50 lb. at 98% efficiency.

The construction of a typical single phase transformer is shown in Figure 21. The transformer consists of a Hiperco wound core, ceramic insulated nickel-clad silver coils and beryllium oxide winding spool. This transformer is not restricted to low temperature or low radiation environments. It rejects its losses either by radiation to space or to a 600°F coolant. For three phase operation, three single phase transformers of this type can be used. The approximate dimensions for these transformers are shown in Tables 10 and 11 and in Figure 21.

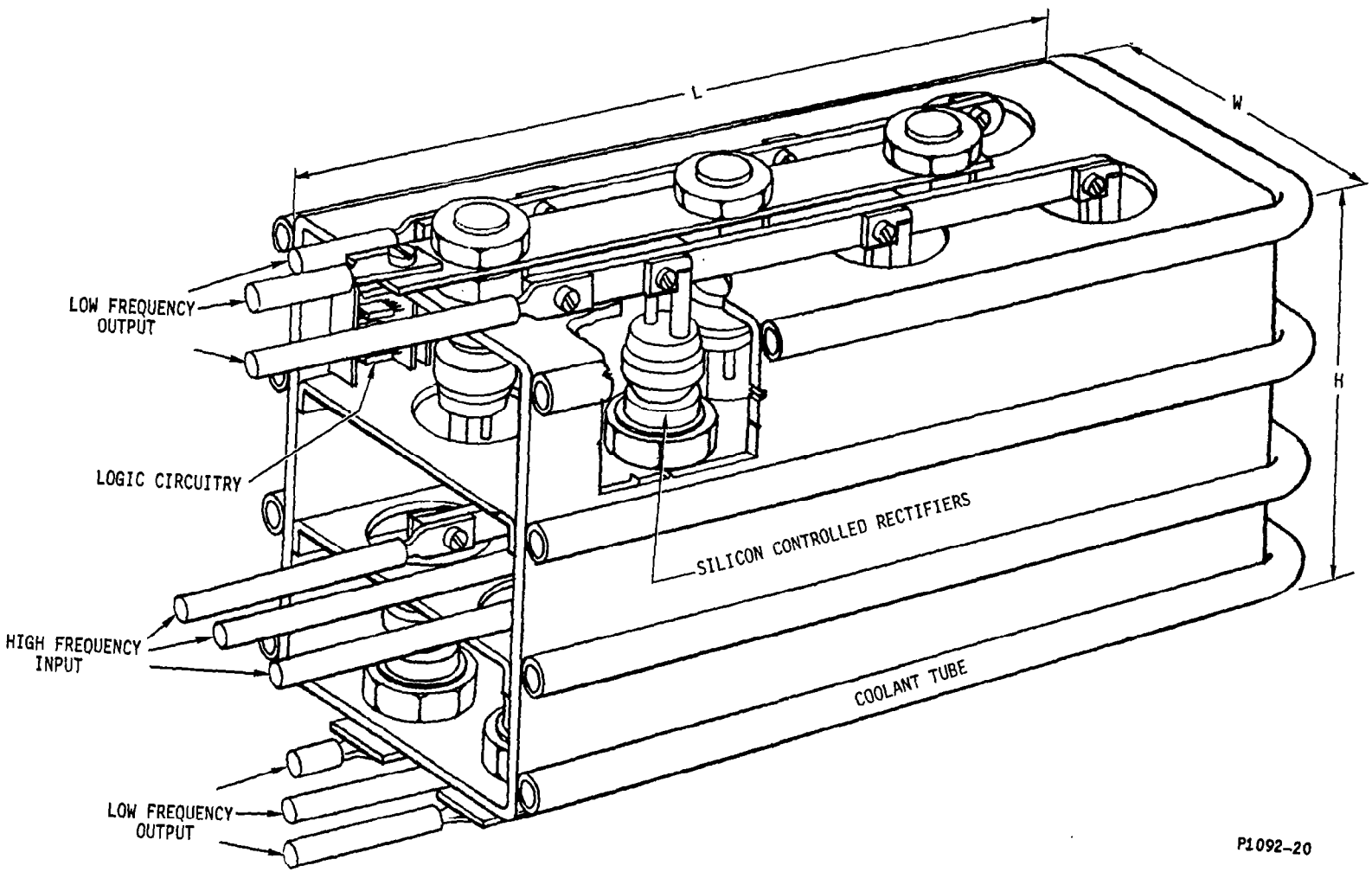

Figure 20. Isometric View Synchronous Static Frequency Divider.

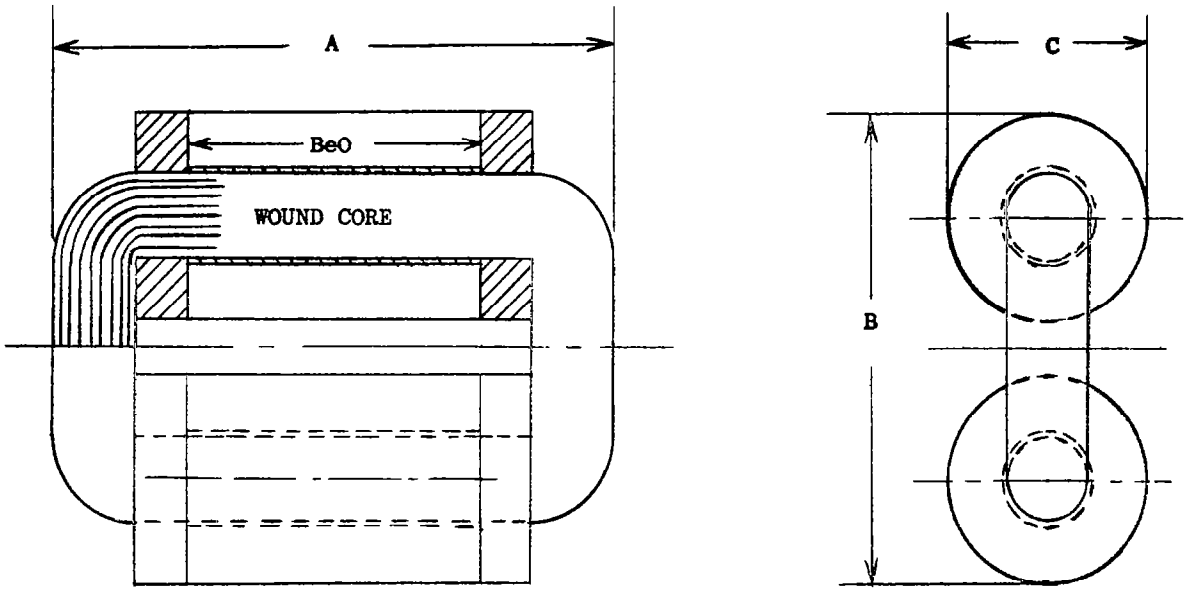

Figure 21. Construction of Single Phase Transformer.

TABLE 14. EQUIVALENT CIRCUIT PARAMETERS

		9 lb/sec Pump (T-111 Duct)	9 lb/sec Pump (316 SS Duct)	3.25 lb/sec Pump (T-111 Duct)
R_i	(ohms)	88.2	98.2	20.6
R_1	(ohms)	0.148	0.148	0.063
X_1	(ohms)	0.816	0.821	0.221
R_c	(ohms)	105	105	25.9
R_{d1}	(ohms)	11.2	18.1	3.35
X_{f1}	(ohms)	0.131	0.125	0.029
R_{f1}	(ohms)	1.10	1.27	0.392
X_{d2}	(ohms)	0.066	0.065	0.014
R_{d2}	(ohms)	18.1	28.4	4.96
X_m	(ohms)	1.35	1.36	0.396
s'		0.425	0.424	0.465
s		0.421	0.424	0.444
I_1	(amps)	121	121	144
V_1	(volts)	242	256	82.9

3. Control of the Pump

The 3.25 lb/sec pump is rated for 32.8 gpm flow rate, 240 psi developed pressure with 1000°F potassium as the working fluid. It is required that the pump be able to operate over relatively wide ranges. Both the flow and the developed pressure can be controlled by varying the input voltage, or by varying both input voltage and frequency.

a. Voltage Control. Voltage control can be accomplished by placing several taps on the transformer. As far as the power conditioning equipment is concerned this is a very efficient control. However, the pump efficiency deteriorates roughly linearly with flow, i.e., low flow corresponds to low efficiency. Another problem associated with a tapped transformer concerns making a switching mechanism which must operate either in hard vacuum or in a hermetically sealed gas. These switches generally do not have high loss but they do add considerable weight and decrease reliability.

Voltage control can also be accomplished by electronically delaying the firing of the SCRs in the frequency divider to provide a smaller rms voltage. This essentially provides the same control as a tapped transformer except it is continuous. This approach eliminates the need for the switching mechanism required by the tapped transformer. The disadvantage of this method is that delaying the firing causes switching losses in the SCRs. For a 400 cps input frequency, the switching loss is estimated to be approximately 350 watts, whereas for a 1200 cps input frequency the switching loss is estimated to be approximately 1000 watts.

b. Voltage and Frequency Control. The logic circuitry can easily be made to yield various frequencies below the 60 cps with negligible weight and efficiency penalties. This could allow the pump to operate at a lower frequency to provide lower flow rates and pressures with efficiencies which might approach the 60 cps design point efficiencies.

V. APPENDIX

A. Performance Calculations - Equivalent Electrical Circuit

Generalized expressions for power output, losses, pump efficiency, developed pressure and other basic characteristics are developed and presented in several references, in particular, References 1, 7, and 8. To design and analyze a specific EM pump these basic expressions have to be related to the stator structure, windings, and detailed dimensional data for the particular configuration being considered. In addition other effects neglected in the generalized expressions such as end effects, flux fringing, iron losses, hydraulic losses and etc. must be properly taken into account. This is most readily done through the use of an equivalent electrical circuit for the EM pump which is the same approach used in induction motor design.

The equivalent circuit used in this design study for each phase of the three helical induction EM pump is shown in Figure 8. Its derivation and solution are analogous to that for an induction motor as presented in several classical texts such as reference 9. The solution of this circuit, is used to determine the complete performance characteristics for any specific helical induction EM pump. Equivalent circuit parameters are calculated in terms of the geometry of the specific pump being analyzed. This calculation of parameters, solution of the equivalent circuit and translation of the circuit solution into pump performance has been programmed for calculation on a digital computer. To determine the three final designs for this study many design variations were run on the computer. Basic design parameters varied were frequency, duct and stator diameters, stator slot and winding geometry, fluid velocity, duct flow passage geometry and stator length. Several hundred computer runs were made for each design required to determine the final design parameters and geometry. For the final helical EM pump designs selected, the equivalent circuit parameters in Figure 8, based on computer calculations, are given in Table 12.

The parameters in the equivalent circuit use symbols defined in the nomenclature. Two items which may require further clarification are the leakage reactance term X_1 and the dimensionless parameter s'. The reactance X_1 consists of stator winding leakage reactance, outer duct wrapper leakage reactance, and winding harmonic leakage reactance.

The dimensionless parameter s' is a function of slip and takes into account the fact that the liquid metal is moving through the helical passage at some slip s, while the duct separators between the helical flow passages are stationary (unity slip). The current in this path flows axially through the moving fluid and the stationary separators. Hence s' can be thought of as an effective slip valve for the fluid and separators in series. In addition s' takes into account an end effect where the liquid metal enters and discharges from the helical passage.

The calculated results shown in Figures 9 through 17 and Tables, 1, 2 and 3 for the final designs were obtained using this equivalent circuit and the associated computer program.

B. Hydraulic Analysis

The computer program for the solution of the equivalent electrical circuit and calculation of performance includes a calculation of hydraulic loss through the pump and factors this into the calculation of overall performance. Basically, the hydraulic pressure drop through the pump duct can be expressed as,

$$P_h = 4\,\delta\,\frac{c}{D_h}\,\frac{\sigma_v^2}{2g} + h\,\frac{\sigma_v^2}{2g} \qquad \text{(B-1)}$$

where the first term represents the friction drop through the helical passage and the second term represents the hydraulic loss, as a number of velocity heads, in entering the helical passage, leaving the helical passage, making a 180° bend into the center return pipe and passing through the center return pipe. Friction factor, δ , depends on Reynolds number and Hartman number which are determined through use of the following basic equations:

$$N_R = \frac{\sigma_v D_h}{\mu}$$

$$N_H = \frac{B_f\, D_h}{4\sqrt{\rho_f \frac{\mu}{g}}}$$

For the final designs using the high velocity portion of the helical ducts, these values become:

	3.25 lb/sec (T-111 Duct)	9 lb/sec (T-111 Duct)	9 lb/sec (316 SS Duct)
D_h (inches)	0.578	0.896	0.884
B_f (k lines/in^2)	13.1	13.7	14.7
N_R	248,000	443,000	438,000
N_H	83	134	142

These data indicate that flow through the helix is turbulent. Entering a curve of δ as a function of $N_R + N_H$ as presented in Reference 1, one determines the friction factor in the duct to be in the range of 0.0034 - 0.0038. To account for curvature and the lower velocity in the first two turns of the helix a slightly conservative value of 0.005 was used in the computer design calculations. The entrance and exit loss factor, h, was estimated as 1.5 velocity heads based

on geometry and past experience with similar type pumps. The resulting net hydraulic loss at 1000°F from the duct inlet to the duct outlet, as determined by computer calculation using equation (B-1), is as follows:

	3.25 lb/sec (T-111 Duct)	9 lb/sec (T-111 Duct)	9 lb/sec (316 SS Duct)
Duct Entrance Loss (psi)	1.8	2.3	2.3
Loss through Helical Passage (psi)	31.6	26.4	24.6
Helix Exit Loss (psi)	1.3	1.8	1.8
180° Bend Loss (psi)	1.6	3.0	3.0
Center Return Pipe & Exit Loss (psi)	.2	.4	.4
Total Hydraulic Loss (psi)	36.5	33.9	32.1

These values were shown in Table 4.

C. Heat Transfer Analysis

Temperature of the stator winding is a principal factor in limiting output. It is a function of the liquid metal and duct temperature, winding current density, cooling system and the geometry and thermal characteristics of the pump structure. The temperature rise of the winding can be determined through the use of an equivalent thermal circuit. Solution of an equivalent thermal circuit for a liquid cooled helical induction pump with a heat exchanger around the frame as in this case has been programmed on a digital computer. The results of calculations at the design point using this program for the final pump designs described in this report were as follows:

	3.25 lb/sec	9 lb/sec
Winding Hot Spot Temperature Rise	275°F	300°F
Winding Average Temperature Rise	170°F	165°F

These results represent the temperature rise above average coolant temperature. For average NaK coolant temperature of 675°F the actual winding temperatures become

	3.25 lb/sec	9 lb/sec
Winding Hot Spot Temperature	950°F	975°F
Winding Average Temperature	845°F	840°F

These results are based on assuming that the entire heat load flows through the stator core to the heat exchanger which is conservative, since some heat will beconvected or radiated from the winding end turns. The accuracy of these results is limited primarily by the accuracy of the thermal resistivities used in the computer program; in particular, the resistivity of the thermal insulation between the duct and stator and the electrical insulation between the conductors and stator iron. These thermal resistivity values among others are tabulated in Appendix E, Design Data and Physical Properties.

The total heat load transmitted to the cooling system consists of the stator losses plus the heat load from the duct through the thermal insulation. For the design point with the liquid metal at 1000°F and an average NaK coolant temperature of 675°F the heat load from the duct, stator losses and total heat load are as follows:

	3.25 lb/sec (T-111 Duct)	9 lb/sec (T-111 Duct)	9 lb/sec (316 SS Duct)
Heat Load From Duct Through Thermal Insulation, KW	0.59	1.12	1.12
Winding (I^2R) Losses, KW	3.85	6.39	6.43
Iron Loss, KW	1.0	2.0	2.0
Total Heat Load, KW	5.44	9.51	9.55

Based on these heat loads the heat exchanger requirements can be established. Typical calculation for the 3.25 lb/sec pump is as follows.

If the average coolant temperature desired is 675°F, then for a coolant inlet temperature of 650°F the outlet temperature must be 700°F giving a coolant temperature rise through the heat exchanger of 50°F. The required NaK coolant flow is given by

$$Q = \frac{3413\ (q_T)}{C_p\ \Delta T} \qquad \text{(C-1)}$$

where

q_T = heat load in KW

C_p = specific heat of NaK in $\frac{Btu}{lb\ °F}$

Q = NaK coolant flow rate in lb/hr

Using a conservative value of 6 KW for the heat load, one calculates

$$Q = \frac{3413\ (6)}{.21\ (50)} = 1950\ \text{lb/hr} \approx 5\ \text{gal/min}$$

This is the minimum required flow for this heat load and temperature rise. For additional design margin and conservatism let us specify 6 gal/min required. For parallel flow with inlet at each end of the heat exchanger and outlet at the center, the recommended minimum flow is 3 gal/min per half. For the given 3.25 lb/sec design, the coolant pressure drop through the heat exchanger is calculated as follows:

Area of coolant flow passage, $A_c = .25 \times .45 = .1125\ \text{in}^2$

Hydraulic diameter, $D_{hc} = \frac{4(.1125)}{1.4} = .322"$

Velocity of coolant, $v_c = \frac{.32(3)}{.1125} = 8.54\ \text{ft/sec}$

Velocity head, $\frac{\sigma_c v_c^2}{2g} = \frac{49.4(8.54)^2}{64.4 \times 144} = .388\ \text{psi}$

Reynolds number, $N_R = \frac{\sigma_c v_c D_{hc}}{\mu_c} = 76{,}800$

For this Reynolds number, the friction factor, δ, is approximately 0.005 which gives a pressure drop through one half the heat exchanger of

$$\Delta P = 4\ \delta \frac{c}{D_{hc}} \frac{\sigma_c v_c^2}{2g} = 8.3\ \text{psi}$$

To account for approximately 1 to 2 velocity heads lost at entrance to and discharge from the helical heat exchanger let us specify 9 psi pressure drop. Therefore, the heat exchanger requirements are a total flow of 6 gpm at 9 psi pressure for a parallel flow heat exchanger as shown in the final designs. A similar calculation was performed for the 9 lb/sec designs to establish their heat exchanger requirements at 8 gpm, 16 psi.

Also of interest is the temperature rise of the primary liquid metal, potassium, through the EM pump duct. For the 3.25 lb/sec pump this is calculated as follows:

$$\Delta T_f = \frac{3413(q_f)}{C_p\ Q_f}$$

where

q_f = total heat generated in duct and fluid less heat conducted through thermal insulation

$$q_f = KW_{d1} + KW_{d2} + KW_f + KW_h - KW_{ti}$$

$$q_f = 2.34 + 1.29 + 4.22 + .52 - .59 = 7.78 \text{ kw}$$

$$\Delta T_f = \frac{3413\ (7.78)}{.181\ (3.25 \times 3600)} = 12.5°F$$

This rise is quite insignificant compared to the 1000°F fluid temperature. By a similar calculation, the rise for each of the 9 lb/sec designs is as follows:

	T-111 Duct	316 SS Duct
q_f	19.33 KW	16.97 KW
ΔT_f	11.3°F	9.9°F

D. Mechanical Design Calculations

This section of the Appendix Contains the Detailed mechanical analysis and calculations required to verify the structural integrity of the 3.25 lb/sec helical EM pump design shown in Figure 1. References 10, 11, 12, 13, 14, 15, 16, 17 and 18 were used in various parts of this analysis.

Identical calculations were also made for the 9 lb/sec design with similar results to those included here.

The calculations are sub-divided as follows the ease of reference:

1. Duct
    a. Outer Wrapper
    b. End Cap
    c. Intermediate Cylinder
    d. Inner Cylinder
    e. Helix
    f. Inlet/Outlet Pipes
2. Frame and Heat Exchanger
    a. Internal Pressure
    b. Outer Shell - Connection End - Inconel
    c. Outer Shell - Hastelloy B
    d. End Shield - Connection End - Inconel
    e. Outer Shell - Opp. Connection End
    f. End Shield - Opp. Connection End
    g. Heat Exchanger
    h. Heat Exchanger Wrapper

The following list of symbols applies to this Appendix section only:

c - Distance of fiber from centroid - inch

D - $EL^3/12\ (1 - \nu^2)$ - inch lb

d - Diameter - inch

E - Modulus of Elasticity - lb/sq in

I - Moment of Inertia - $(inch)^4$

M_o - Moment at End - inch lb/inch

m - $1/\nu$

P - Pressure - psi

R,r - Radius - inch

T - Temperature - °F

t - Thickness - inch

V_o - Shear Force at End - lb/inch

α - Coefficient of thermal expansion - in/in/°F

β - $[3(1-\nu 2) / R^2t^2]^{1/4}$ - $(inch)^{-1}$

δ - Deflection or expansion - inch

$\Delta\delta$ - Differential deflection or expansion - inch

λ - Identical to β

ν - Poisson's ratio - dimensionless

σ - Stress - psi

Subscripts

1 - Refers to head

2 - Refers to shell

H - Hastelloy

h - Hoop (stress)

I - Inconel

i - Inside (radius)

ℓ - Longitudinal (Stress)

0 - Outside (radius)

P - Punching

r - Radial (stress)

t - Tangential (stress)

1. Duct

The duct material is T-111 alloy. At the design temperature of 1300°F, the 10,000 hour stress rupture value is over 80,000 psi. Thus, the design thicknesses are limited by fabrication considerations rather than by stress values.

a. Outer Wrapper

(1) Primary Pressure Stress

From Reference 10, the longitudinal membrane stress is:

$$\sigma_\ell = \frac{PR}{2t} = \frac{350 \times 2.019}{2 \times .062} \qquad \text{(D-1)}$$

$$\sigma_\ell = 5699 \text{ psi}$$

The hoop stress is:

$$\sigma_h = 2\,\sigma_\ell = 11{,}398 \text{ psi}$$

(2) Stress Due to Shrink Fit of Wrapper Over Helix

The wrapper will be assembled over the helix with an approximate 0.002 inch interference fit. From Reference 10, this radial displacement is:

$$\delta = \frac{R}{E}\,(\sigma_h - \nu\sigma_\ell) \qquad \text{(D-2)}$$

and $\sigma_h = 2\sigma_\ell$ Thus,

$$\delta = R/E\,(2-\nu)\sigma_\ell$$

Substituting known values:

$$.002 = \frac{2.019 \times 1.7}{24.8 \times 10^6}\ \sigma_\ell$$

$$\sigma_\ell = 14{,}451 \text{ psi}$$

$$\sigma_h = 28{,}902 \text{ psi}$$

(3) Stress Due to Discontinuity at End Cap

From Reference 10 the moment due to the discontinuity is:

$$M_o = \frac{\left[\frac{PR^3 \lambda^2 D_2}{4D_1 (1+\nu)} + \frac{2 PR^2 \lambda^3 Et_1 D_2}{Et_2 (1-1/2\ \nu)\ [Et_1 + 2 R D_2 \lambda^3 (1-\nu)]}\right]}{\left[2\lambda + \frac{2 R \lambda^2 D_2}{D_1 (1+\nu)} - \frac{\lambda Et_1}{Et_1 + 2 D_2 \lambda^3 R (1-\nu)}\right]} \qquad \text{(D-3)}$$

where:

$$\lambda = \sqrt[4]{\frac{3(1-\nu^2)}{R^2 t^2}} = 3.6331 \qquad \text{(D-4)}$$

$$D = \frac{Et^3}{12(1-\nu^2)} \qquad \text{(D-5)}$$

$$D_1 = 283{,}883$$

$$D_2 = 541.26$$

Substituting known values:

$$M_o = 18.8275 \text{ in-lb/in}$$

$$V_o = M_o \left[2\lambda + \frac{2 R \lambda^2 D_2}{D_1 (1+\nu)}\right] - \frac{PR^3 \lambda^2 D_2}{4 D_1 (1+\nu)} \qquad \text{(D-6)}$$

$$V_o = 124.335 \text{ lb/in}$$

The stresses due to these reactions are:

Moment

$$\sigma_{\ell} = \frac{-6\ M_o}{t^2} = -29{,}387 \text{ psi} \qquad \text{(D-7)}$$

$$\sigma_h = \frac{2\ M_o\ \lambda^2\ R}{t} = 16{,}185 \text{ psi} \qquad \text{(D-8)}$$

Force

$$\sigma_{\ell} = \frac{1.932\ V_o}{\lambda t^2} = 17{,}201 \text{ psi} \qquad \text{(D-9)}$$

$$\sigma_h = \frac{-2\ V_o\ \lambda\ R}{t} = 29{,}420 \text{ psi} \qquad \text{(D-10)}$$

(4) Stress Due to Discontinuity at Connector

As the worst case, the outer wrapper will be assumed to be built in. Thus, from Reference 12:

$$M_o = P/2\ \beta^2 \qquad \text{(D-11)}$$

$$V_o = P/\beta \qquad \text{(D-12)}$$

$$\beta = \sqrt[4]{\frac{3\ (1-\nu^2)}{R^2\ t^2}} = 3.6331 \qquad \text{(D-13)}$$

At P = 350 psi,

M_o = 13.26 in lb/in

V_o = -96.34 lb/in

And

$$\sigma_t = \frac{6(1-\nu^2)}{\beta^2\ t^2\ R}\left[\frac{V_o}{\beta} + M_o\right] \pm \nu\sigma_{\ell} \qquad \text{(D-14)}$$

$$\sigma_{\ell} = \pm \frac{6\ M_o}{t^2} \qquad \text{(D-15)}$$

Substituting known quantities:

σ =	At OD	At ID
	-21,401	20,694
σ_t =	-21,401	19,988

(5) Stress Summary - Duct Outer Wrapper

Helix Area

	σ_ℓ	σ_h
Pressure	5,699	11,398
Shrink Fit	14,451	28,902

These stresses are interdependent and not combined. As the pressure increases, the shrink decreases as do their stress components.

At End Cap

	σ_ℓ	σ_h
Primary Pressure	5,699	11,398
Secondary Moment	-29,387	16,185
Secondary Force	17,201	-29,420
Total (Primary and Secondary)	-6,488	- 1,837

At Connector

At OD

	σ_ℓ	σ_h
Primary Pressure	5,699	11,398
Secondary Bending	-20,694	-21,401
Total (Primary and Secondary)	-14,996	-10,004

At ID

	σ_ℓ	σ_h
Primary Pressure	5,699	11,398
Secondary Bending	20,694	19,988
Total (Primary and Secondary)	26,391	31,385

These stress values are within acceptable limits.

b. End Cap

(1) Primary Pressure Stress

The stress values for a circular plate, edges supported with a uniform load over the entire surface are given in Reference 10 as:

$$\sigma_r = \frac{-3\ P\ r_a^{\ 2}}{8\ m\ t^2}\left[(3\ m + i)\left(1 - \frac{r^2}{r_o^{\ 2}}\right)\right] \qquad \text{(D-16)}$$

and

$$\sigma_t = \frac{-3\ P\ r_o^{\ 2}}{8\ m\ t^2}\left[(3\ m + i) - (m + 3)\frac{r^2}{r_o^{\ 2}}\right] \qquad \text{(D-17)}$$

At the plate center, the stresses are a maximum, r = o,

$\sigma_r = \sigma_t = -7{,}062$ psi

At the plate OD, $r = r_o$

$\sigma_r = o$

$\sigma_t = -2{,}996$ psi

(2) Stress Due to Discontinuity at Outer Wrapper

From before, the reactions are

$M_o = 18.8275$ in-lb/in

$V_o = 124.335$ lb/in

The stresses resulting from these reactions are:

Moment

$$\sigma_r = \sigma_t = \frac{6M}{t^2} = -452 \text{ psi}$$

Force

$\sigma_t = 0$

$\sigma_r = V_o/t = 249$ psi

(3) Stress Summary - Duct End Cap

At Center

	σ_r	σ_t
Primary Pressure	-7,062	-7,062
Secondary Moment	-452	-452
Secondary Force	249	0
Total (Primary and Secondary)	-7,265	-7,514

At OD

	σ_r	σ_t
Primary Pressure	0	-2,996
Secondary Moment	-452	-452
Secondary Force	249	0
Total	-203	-3,448

These stress values are within acceptable limits.

c. Intermediate Cylinder

(1) Primary Pressure Stress

$$\sigma_\ell = \frac{PR}{2t} = \frac{-240 \times 1.308}{2 \times .06} \qquad \text{(D-18)}$$

$$\sigma = -2616 \text{ psi}$$

$$\sigma_t = 2\,\sigma_\ell = -5232 \text{ psi}$$

(2) Stress Due to Bending of Separators

The moment caused by the bending of the separator is

M = 23.099 in-lb or 2.7476 in-lb/in

The stress in the cylinder due to this moment is, from Reference 10:

$$\sigma_\ell = \frac{-6M_o}{t^2} = \frac{-6 \times 2.7476}{(.06)^2} \qquad \text{(D-19)}$$

$$\sigma_\ell = \pm 4,579 \text{ psi}$$

$$\sigma_h = \frac{2\, M_o\, \lambda^2\, R}{t} \qquad \text{(D-20)}$$

$$\lambda^2 = \sqrt{\frac{3(1-\nu^2)}{R^2\, t^2}} = 21.05 \qquad \text{(D-21)}$$

$$\sigma_h = \pm \frac{2 \times 2.7476 \times 21.05 \times 1.308}{.06} = 2523 \text{ psi}$$

(3) End Reaction

For a cylinder with fixed ends, external pressure, Reference 15 gives the reactions as:

$$M_o = P/2\,\beta^2 = -5.70 \text{ in-lb/in} \qquad \text{(D-22)}$$

$$V_o = -P/\beta = 52.306 \text{ lb/in} \qquad \text{(D-23)}$$

The stresses due to these reactions are:

	At OD	At ID
σ_ℓ	9,500	-9,500
σ_t	9,814	-9,168

(4) Stress Summary - Duct Intermediate Cylinder

Under Helix	σ_ℓ	σ_h
Pressure	-2,616	-5,232
Moment	±4,579	±7,755
Total	-7,195	-12,987

At Ends - ID	σ_ℓ	σ_h
Primary Pressure	- 2,616	- 5,232
Secondary Bending	- 9,500	- 9,186
Total	-12,116	-14,118

At Ends - OD	σ_ℓ	σ_h
Primary Pressure	-2,616	-5,232
Secondary Bending	+9,500	+9,814
Total	6,884	4,582

These stress values are within acceptable limits.

d. Inner Cylinder - Duct

(1) Primary Pressure Stress

$$\sigma_\ell = \frac{PR}{2t} = \frac{240 \times .815}{2 \times .06} = 1{,}834 \text{ psi} \qquad \text{(D-24)}$$

$$\sigma_h = 2\,\sigma_\ell = 3{,}668 \text{ psi} \qquad \text{(D-25)}$$

(2) End Reaction

$$\beta = \sqrt[4]{\frac{3(1-\nu^2)}{R^2\,t^2}} = 5.8128 \qquad \text{(D-26)}$$

$$M_o = P/2\beta^2 = 3.995 \text{ in-lb/in} \qquad \text{(D-27)}$$

$$V_o = P/\beta = -46.449 \text{ lb/in} \qquad \text{(D-28)}$$

The stresses due to these reactions are:

	At OD	At ID
σ_ℓ	-6,659	6,659
σ_h	-6,879	6,439

(3) Stress Summary - Duct Inner Cylinder

At OD	σ_ℓ	σ_h
Primary Pressure	1,834	3,668
Secondary Bending	-6,659	-6,879
Total	-4,825	-3,211
At ID	σ_ℓ	σ_h
Primary Pressure	1,834	3,668
Secondary Bending	6,659	6,439
Total	8,493	10,107

These stress values are within acceptable limits.

e. Helix

As a worst case, it will be assumed that the thread lead is constant at 0.85 inch.

The differential pressure across each separator is:

$$\Delta P = \frac{P \times \text{lead}}{\text{Length}} = \frac{240 \times 0.85}{13} \qquad \text{(D-29)}$$

$$\Delta P = 15.692 \text{ psi}$$

The separator is essentially a cantilever beam. The pressure causes a maximum moment of:

$$M = \Delta P \pi \left(\frac{d_o + d_i}{2}\right)\left(\frac{d_o - d_i}{2}\right)\left(\frac{d_o - d_i}{4}\right) \qquad \text{(D-30)}$$

$$M = 15.692\pi\ (2.217)(.65)(.325) - 23{,}099 \text{ in-lbs}$$

$$C = t/2 = .05/2 = .025 \text{ in} \qquad \text{(D-31)}$$

$$I = bd^3/12 = 1/12\left[\pi\left(\frac{d_o + d_i}{2}\right) t^3\right] = 1.4417 \times 10^{-5} \qquad \text{(D-32)}$$

$$\sigma = \frac{M_c}{I} = 27{,}211 \text{ psi} \qquad \text{(D-33)}$$

This stress is within acceptable limits.

f. Inlet/Outlet Pipes

(1) Primary Pressure

$$\sigma_\ell = \frac{PR}{2t} = \frac{350 \times .603}{2 \times .109} = 968 \qquad \text{(D-34)}$$

$$\sigma_h = 2\sigma_\ell = 1936 \qquad \text{(D-35)}$$

(2) End Reaction

$$\beta = \sqrt[4]{\frac{3(1-\nu^2)}{R^2\ t^2}} = 5.0138 \qquad \text{(D-36)}$$

$$M_o = P/2\beta^2 = 6.9615 \text{ in-lb/in} \qquad \text{(D-37)}$$

$$r_o = -P/\beta = -69.807 \text{ lb/in} \qquad \text{(D-38)}$$

The stresses due to these reactions are:

	At OD	At ID
σ_ℓ	-3,516	3,516
σ_h	-3,727	3,305

(3) Stress Summary - Duct Inlet/Outlet Pipes

At OD	σ_ℓ	σ_h
Primary Pressure	968	1,936
Secondary Bending	-3,516	-3,727
Total	-2,548	-1,791

At ID	σ_ℓ	σ_h
Primary Pressure	968	1,936
Secondary Bending	3,516	3,305
Total	4,484	5,241

These stress values are within acceptable limits.

2. Frame and Heat Exchanger

The maximum stress values used in this section are, based on 900°F

Material	σ_{max}	σ_y (.2%)	Reference
Inconel	14,900	69,200	14 & 18
Hastelloy B	16,600	39,300	16 & 17

a. Internal Pressure

The pump frame will be filled with inert gas to 6-9 psia at room temperature. During operation, this gas will become heated to a maximum of 900°F. This will result in a corresponding pressure of:

$$P_o = P_R \frac{T_o}{T_R} = 9 \frac{(900 + 460)}{(70 + 460)} \qquad \text{(D-39)}$$

$$P_o = 23.2 \text{ psia}$$

Since this pump is designed to operate in a vacuum, the design pressure will be:

$$P = 25 \text{ psi}$$

b. Outer Shell - Connection End - Inconel

$$\sigma_\ell = \frac{PR}{2t} = \frac{25 \times 5.3125}{2 \times .125} = 531 \qquad \text{(D-40)}$$

$$\sigma_h = 2\sigma_\ell = 1062 \qquad \text{(D-41)}$$

(2) Reaction at End Shield

$$\lambda = \sqrt[4]{\frac{3(1-\nu^2)}{R^2 t^2}} = 1.5774 \qquad \text{(D-42)}$$

$$D = \frac{Et^3}{12(1-\nu^2)} \qquad \text{(D-43)}$$

$D_1 = 34{,}341; \quad D_2 = 4{,}293$

$$M_o = \frac{\left[\frac{PR^3 \lambda^2 D_2}{4D_1 (1+\nu)} + \frac{2 P R^2 \lambda^3 Et_1 D_2}{Et_2 (1-1/2 \nu) \left[Et_1 + 2 R D_2 \lambda^3 (1 - \nu)\right]}\right]}{\left[2\lambda + \frac{2 R \lambda^2 D_2}{D_1 (1 + \nu)} - \frac{\lambda Et_1}{Et_1 + 2 D_2 \lambda^3 R (1-\nu)}\right]} \qquad \text{(D-44)}$$

Substituting known values

$$M_o = 56.201 \text{ in-lb/in}$$

$$V_o = M_o \left[2\nu + \frac{2 R \lambda^2 D_2}{D_1 (1 + \nu)}\right] - \frac{PR^3 \lambda^2 D_2}{4 D_1 (1 + \nu)} \qquad \text{(D-45)}$$

$$V_o = 95.968 \text{ lb/in}$$

The stresses due to these reactions are:

Moment

$$\sigma_{\ell} = \frac{-6\ M_o}{t^2} = -21,581 \qquad \text{(D-46)}$$

$$\sigma_h = \frac{2\ M_o\ \lambda^2\ R}{t} = 11,886 \qquad \text{(D-47)}$$

Force

$$\sigma_{\ell} = \frac{1.932\ V_o}{\lambda\ t^2} = 7,523 \qquad \text{(D-48)}$$

$$\sigma_h = \frac{-2\ V_o\ \lambda\ R}{t} = -12,867 \qquad \text{(D-49)}$$

(3) Reaction at Hastelloy B Junction

A thermal stress is generated at the junction of the Inconel and Hastelloy B due to the different coefficients of thermal expansion. This differential expansion is

$$\Delta\delta = \Delta\ T\ R\ (\alpha_I - \alpha_H) \qquad \text{(D-50)}$$

$$\Delta\delta = 830 \times 5.3125\ (8.2 - 6.6)\ 10^{-6}$$

$$\Delta\delta = 7.055 \times 10^{-3} \text{ inch}$$

Each of the two cylinders will be deflected a portion of this expansion, in proportion to their moduli of elasticity. Thus:

$$\delta_I = \left(\frac{24}{24 + 24.8}\right)\ 7.055 \times 10^{-3} = 3.4696 \times 10^{-3}$$

$$\delta_H = 3.5854 \times 10^{-3}$$

From Reference 12:

$$M_o = 2\ \lambda^2\ D\ \delta = 73.825 \text{ in-lb/in} \qquad \text{(D-51)}$$

$$V_o = 2\ \lambda\ M_o = -231.55 \text{ lb/in} \qquad \text{(D-52)}$$

The resultant stresses are:

Moment

$$\sigma_\ell = 6\ M_o/t^2 \qquad = -28,373 \qquad \text{(D-53)}$$

$$\sigma_h = 2\ M_o\ \lambda^2\ R/t = \ 15,551 \qquad \text{(D-54)}$$

Force

$$\sigma_\ell = \frac{1.932\ V_o}{\lambda t^2} \qquad = -18,130 \qquad \text{(D-55)}$$

$$\sigma_h = 2\ V_o\ \lambda R/t \qquad = +31,046 \qquad \text{(D-56)}$$

(4) Stress Summary - Outer Shell - Connection End - Inconel

At End Shield

	σ_ℓ	σ_h
Primary Pressure	531	1,062
Secondary Moment	-21,581	11,886
Secondary Force	7,523	-12,867
Total	-13,527	81

At Hastelloy B

	σ_ℓ	σ_h
Primary Pressure	531	1,062
Thermal Moment	-28,373	15,551
Thermal Force	-18,150	31,046
Total	-45,992	47,659

The stress values are within acceptable limits. The high stress at the Hastelloy B junction is mainly a thermal stress and the Inconel will withstand about 2000 cycles of this magnitude, based on a fatigue evaluation.

c. Outer Shell - Hastelloy B

(1) Primary Pressure Stress

From Equations (D-40) and (D-41):

σ_ℓ = 531 psi

σ_h = 1,062 psi

(2) Reaction at Inconel Junction

The moment and force will be equal and opposite to those in the inconel shell. Thus,

M_o = 73.825

V_o = 231.55

Since the material thicknesses and Poisson's ratios are the same, the stresses will be equal, but opposite:

Moment

σ_ℓ = 28,373

σ_h = -15,551

Force

σ_ℓ = 18,150

σ_h = -31,046

(3) Reaction at Heat Exchanger

For conservatism, the heat exchanger will be treated as fixed. Thus,

$$\beta = \sqrt[4]{\frac{3(1-\nu^2)}{R^2 t^2}} = 1.5774 \qquad \text{(D-57)}$$

$$M_o = P/2\ \beta^2 = 5.0239 \qquad \text{(D-58)}$$

$$V_o = P/\beta = -15.849 \qquad \text{(D-59)}$$

The resultant stresses are:

$$\sigma_t = \frac{6(1-\nu^2)}{\beta^2 t^2 R}\left[\frac{V_o}{P} + M_o\right] \pm \nu\sigma_\ell \qquad \text{(D-60)}$$

$$\sigma_\ell = \pm 6\, M_o/t^2 \qquad \text{(D-61)}$$

Substituting known quantities:

	At OD	At ID
σ_ℓ	-1,929	1,929
σ_h	-2,062	1,796

(4) Stress Summary - Outer Shell - Hastelloy B

At Inconel

	σ_ℓ	σ_h
Primary Pressure	531	1,062
Thermal Moment	28,373	-15,551
Thermal Force	18,150	-31,046
Total	47,053	45,535

At Heat Exchanger

	σ_ℓ	σ_h
Primary Pressure	531	1,062
Secondary Bending	1,929	1,796
Total - ID	2,460	2,858

These stress values are within acceptable limits.

d. End Shield - Connection End - Inconel

(1) Primary Pressure Stress

The stress values for a circular plate, edges supported, with a uniform load over the entire surface are given in Reference 10 as:

$$\sigma_r = \frac{-3Pr_o^2}{8\ m\ t^2}\left[(3\ m+1)\left(1 - \frac{r^2}{r_o^2}\right)\right] \qquad \text{(D-62)}$$

and

$$\sigma_t = \frac{-3Pr_o^2}{8\ m\ t^2}\left[(3\ m+1) - (m+3)\frac{r^2}{r_o^2}\right] \qquad \text{(D-63)}$$

At the plate center, the stresses are a maximum, r = o

$\sigma_r = \sigma_t = -13{,}970$ psi

At the plate OD, $r = r_o$

$\sigma_r = 0$

$\sigma_t = -5{,}927$ psi

(2) End Reaction

From before:

$M_o = 56.201$

$V_o = 95.968$

The resultant stresses are

Moment

$\sigma_r = \sigma_t = 6\ M/t^2 = -5{,}395$

Force

$\sigma_t = 0$

$\sigma_r = V_o/t = 384$

(3) Stress Summary - End Shield - Connection End - Inconel

At ID

	σ_r	σ_t
Primary Pressure	-13,970	-13,970
Secondary Moment	- 5,395	- 5,395
Secondary Force	384	0
Total	-18,982	-19,365

At OD

	σ_r	σ_t
Primary Pressure	0	- 5,927
Secondary Moment	- 5,395	- 5,395
Secondary Force	384	0
Total	- 5,011	-11,322

These stress values are within acceptable limits.

e. Outer Shell - Opposite Connection End

(1) Primary Pressure Stress

$$\sigma_\ell = PR/2t = \frac{25 \times 5.3125}{2 \times .125} = 531 \qquad \text{(D-64)}$$

$$\sigma_h = 2\sigma_\ell = 1{,}062 \qquad \text{(D-65)}$$

(2) Reaction at End Shield

$$\lambda = \sqrt[4]{\frac{3(1-\nu^2)}{R^2\ t^2}} \approx 1.5774 \qquad \text{(D-66)}$$

$$D = \frac{Et^3}{12(1-\nu^2)} \qquad \text{(D-67)}$$

$D_1 = 115{,}900$, $D_2 = 4{,}293$

Using the same type analysis as before:

$M_o = 32.149$

$V_o = 59.210$

The resultant stresses are:

	Moment	Force
σ_ℓ =	12,345	4,641
σ_h =	6,799	-7,939

(3) Reaction at Hastelloy B Junction

These stresses will be identical with those at the connection end.

(4) Stress Summary - Outer Shell - Opposite Connection End

	σ_ℓ	σ_h
Primary Pressure	531	1,062
Secondary Moment	-12,345	6,799
Secondary Force	4,641	-7,939
Total	- 7,173	- 77

These stress values are within acceptable limits.

f. End Shield - Opposite Connection End

(1) Primary Pressure Stress

From Reference 14 the maximum stress is:

$$\sigma_{max} = \sigma_t = \frac{-3P}{4\,m\,t^2\,(r_o^2 - r_i^2)} \left[r_o^4\,(3\,m+1) + r_i^4\,(m-1) - 4\,m\,r_o^2\,r_i^2 - 4(m+1)\,r_o^2\,r_i^2 \ell_n\, r_o/r_i \right] \quad \text{(D-68)}$$

Substituting known values:

σ_{max} = -12,260 psi

(2) End Reactions

These reductions are:

M_o = 32.149

V_o = 59.21

From 2.2, for moment

$$\sigma_r = \frac{6\,M_o r_o^2}{t^2\,(r_o^2 - r_i^2)} \left[1 - \frac{r_i^2}{r^2} \right] \quad \text{(D-69)}$$

$$\sigma_t = \frac{6 M_o r_o^2}{t^2 (r_o^2 - r_i^2)} \left[1 + \frac{r_i^2}{r^2} \right] \qquad \text{(D-70)}$$

Substituting known quantities:

At $r = r_o$

$\sigma_r = 1{,}375$

$\sigma_t = 1{,}929$

At $r - r_i$

$\sigma_r = 0$

$\sigma_t = 3{,}304$

Force

$\sigma_r = V_o/t = 158$

$\sigma_t = 0$

(3) Stress Summary - End Shield - Opposite Connection End

At $r = r_o$

	σ_r	σ_t
Primary Pressure	-12,260	-12,260
Secondary Moment	1,375	1,929
Secondary Force	158	0
Total	-10,727	-10,331

At $r = r_i$

	σ_r	σ_t
Primary Pressure	-12,260	-12,260
Secondary Moment	0	3,304
Secondary Force	158	0
Total	-12,102	- 8,956

These stresses are within acceptable limits.

g. Heat Exchanger

(1) Differential Thermal Expansion Between Heat Exchanger and Stator Punchings

Assuming a ΔT Of 650°F, the differential expansion is:

$$\Delta\delta = R\ \Delta T\ (\alpha_H - \sigma_P) \qquad \text{(D-71)}$$

$$\Delta\delta = 5.3125 \times 650\ (6.5 - 5.95) \times 10^{-6} = 1.9 \times 10^{-3} \text{ in}$$

Stress Due to Differential Thermal Expansion

These stresses must be evaluated under two conditions; non-operating or room temperature and operating. These two conditions impose differing methods of loading on the heat exchanger.

At room temperature, the main loading is due to the interference fit. In addition, the pressure is external at about 7-8 psi. Since this pressure is opposite to that caused by the interference fit, it will be neglected.

Assume shrink fit of 5×10^{-3} inch

$$\delta = \frac{R}{E}\ (2-\nu)\ \sigma_\ell \qquad \text{(D-72)}$$

Solving for σ_ℓ

$$\sigma_\ell = 15{,}074 \text{ psi}$$

$$\sigma_h = 2\sigma_\ell = 30{,}148$$

Under operating conditions, the stress due to the interference fit will be greatly reduced due to the greater expansion of the heat exchanger.

(3) Summary - Heat Exchanger

Some yielding of the heat exchanger may occur during assembly; however, under these circumstances, the stresses would be relieved. Any sustained stress or yield would not affect the operation of the pump. Thus, these stresses are acceptable.

h. Heat Exchanger Wrapper

(1) Interference Fit

Assume 2×10^{-3} inch interference fit:

$$\sigma_\ell = E\delta/R(2-\nu) = 6{,}030 \text{ psi} \qquad \text{(D-73)}$$

$$\sigma_h = 12{,}060 \text{ psi}$$

(2) Internal Pressure

$\sigma_\ell = PR/2t = 544$ (D-74)

$\sigma_h = 2\sigma_\ell = 1,088$ (D-75)

(3) End Reactions

Using the method of Reference 12:

$\beta = 1.559$

$M_o = 5.142$

$V_o = -16.034$

The resulting stresses are:

	At OD	At ID
σ_ℓ	-1,975	1,975
σ_h	-2,110	1,839

(4) Stress Summary - Heat Exchanger Wrapper

At ID

	σ_ℓ	σ_h
Primary Pressure	544	1,088
Secondary Bending	1,975	1,938
Total	2,518	2,926

At OD

	σ_ℓ	σ_h
Primary Pressure	544	1,088
Secondary Bending	-1,975	-2,110
Total	-1,431	-1,023

These stress values are within acceptable limits.

E. Design Data and Physical Properties

(References 1-6, 15, 16, 18, 19 & 20)

	900°F	1000°F	1300°F
1. Potassium Properties			
a. electrical resistivity, ($\mu\Omega$ in)	16.9	18.9	26.3
b. density, (lb/ft^3)	45.4	44.5	42.1
c. specific heat, (Btu/lb°F)	0.182	0.181	0.184
d. thermal conductivity, (watts/°F in)	0.533	0.513	0.455
e. viscosity, (lb/hr ft)	0.45	0.41	0.335
2. Duct Properties - T-111 alloy			
a. electrical resistivity ($\mu\Omega$ in)	17.1	17.9	19.7
b. density (lb/in^3)	0.6	0.6	0.6
c. thermal conductivity (w/°F in)	0.9	0.9	0.9
d. thermal coefficient of expansion (in/in °F) (from room temperature)	4.1×10^{-6}	4.2×10^{-6}	4.3×10^{-6}
3. Duct Properties - 316 stainless steel			
a. electrical resistivity ($\mu\Omega$ in)	41.2	42.6	47.1
b. density (lb/in^3)	0.28	0.28	0.28
c. thermal conductivity (w/°F in)	0.306	0.317	0.35
d. thermal coefficient of expansion (in/in°F) (from room temperature)	9.3×10^{-6}	9.4×10^{-6}	9.8×10^{-3}

4. Winding Properties

a. effective electrical resistivity of conductor @ 880°F (Ni-clad Ag)	2.09 μΩ in
b. density of conductor	0.367 lb/in^3
c. effective thermal conductivity of conductor @ 880°F	8.15 w/°C in
d. effective thermal resistivity of electrical insulation (ceramic and gas)	75 °C in/w

5. Magnetic Material Properties (Hiperco 27)

a. density	0.285 lb/in^3
b. thermal resistivity	0.875 °C in/watt
c. core loss factor at 60 cps; .025" thick lamination	5 watts/lb
d. thermal coefficient of expansion (77°-800°F)	5.96×10^{-6} in/in °F

6. Other Design Data and Properties

a. density of Inconel	0.31 lb/in^3
b. density of Hastelloy B	0.33 lb/in^3
c. electrical resistivity of Inconel can @ 900°F	41 μΩ in
d. thermal resistivity of foil thermal insulation	200°C in/watt
e. thermal coefficient of expansion of Hastelloy B (32°-600°F)	6.4 in/in °F
f. thermal coefficient of expansion of Inconel (32°-600°F)	7.5×10^{-6} in/in°F

7. NaK Properties (as coolant)

a. density @ 700°F	49.4 lb/ft^3
b. specific heat @ 700 °F	0.21 Btu/lb °F
c. viscosity @ 700 °F	0.53 lb/hr ft

REFERENCES

1. Verkamp, J.P. and Rhudy, R.G., "Electromagnetic Alkali Metal Pump Research Program," Report NASA CR-380, Contract NAS 3-2543, General Electric Company, February 1966.

2. Pendleton, W.W., "Radiation-Resistant Magnet Wire for Use in Air and Vacuum at 850°C," Technical Documentary Report ASD-TDR-63-164, Contract AF 33(657)-7473, Anaconda Wire and Cable Company, July 1963.

3. Kueser, P.E., et cl., "Development and Evaluation of Magnetic and Electrical Materials Capable of Operating in the 800°F to 1600°F Temperature Range," Report NASA CR-54354, First Quarterly Report, Contract NAS 3-6465, Westinghouse Electric Corporation, March 1965.

4. Kueser, P.E., et al., "Development and Evaluation of Magnetic and Electrical Materials Capable of Operating in the 800°F to 1600°F Temperature Range," Report NASA CR-54355, Second Quarterly Report, June 1965.

5. Kueser, P.E., et al., "Magnetic Materials Topical Report," Report NASA CR-54091, Contract NAS 3-4162, Westinghouse Electric Corporation, September 1964.

6. Kueser, P.E., et al., "Electrical Conductors and Electrical Insulation Materials Topical Report," Report NASA CR-54092, Contract NAS 3-4162, Westinghouse Electric Corporation, October 1964.

7. Blake, L.R., "Conduction and Induction Pumps for Liquid Metals," Proc. IEE, Part A, Vol. 104, No. 13, February 1957.

8. Watt, D.A., "The Design of Electromagnetic Pumps for Liquid Metals," Paper No. 2763, IEE, December 1958.

9. Alger, P.S., "The Nature of Polyphase Induction Machines," John Wiley & Sons, Inc., 1951.

10. Roark, R.J., "Formulas for Stress and Strain," McGraw-Hill Book Company, Inc., 1943.

11. Marks, L.S., "Mechanical Engineering Handbook," McGraw-Hill Book Company, Inc., New York.

12. Timoshenko, S., "Theory of Plates and Shells," McGraw-Hill Book Company, Inc., 1959.

13. ASME Boiler and Pressure Vessel Code, Section III, "Nuclear Vessels", 1965 Edition.

14. ASME Boiler and Pressure Vessel Code, Section VIII, "Unfired Pressure Vessels," 1965 Edition.

15. Special Technical Data 52-365, "T-111, Tantalum Base Alloy Refractory Metal," Westinghouse Electric Corporation, 1963.

16. "Hastelloy Alloy B", Haynes Stellite Company, 1962.

17. ASME Boiler and Pressure Vessel Code, Code Case 11348.

18. International Nickel Company, "Engineering Properties of Inconel," 1963.

19. Lyon, R.N., Ed., "Liquid Metals Handbook," Revised, Second Edition, U.S. Government Printing Office, Washington, D.C.

20. Jackson, C.B., Ed., "Liquid Metals Handbook-Sodium (NaK) Supplement," Third Edition, U.S. Government Printing Office, Washington, D.C.

NASA-Langley, 1967 —— 15 E-4047

"The aeronautical and space activities of the United States shall be conducted so as to contribute . . . to the expansion of human knowledge of phenomena in the atmosphere and space. The Administration shall provide for the widest practicable and appropriate dissemination of information concerning its activities and the results thereof."

—NATIONAL AERONAUTICS AND SPACE ACT OF 1958

NASA SCIENTIFIC AND TECHNICAL PUBLICATIONS

TECHNICAL REPORTS: Scientific and technical information considered important, complete, and a lasting contribution to existing knowledge.

TECHNICAL NOTES: Information less broad in scope but nevertheless of importance as a contribution to existing knowledge.

TECHNICAL MEMORANDUMS: Information receiving limited distribution because of preliminary data, security classification, or other reasons.

CONTRACTOR REPORTS: Scientific and technical information generated under a NASA contract or grant and considered an important contribution to existing knowledge.

TECHNICAL TRANSLATIONS: Information published in a foreign language considered to merit NASA distribution in English.

SPECIAL PUBLICATIONS: Information derived from or of value to NASA activities. Publications include conference proceedings, monographs, data compilations, handbooks, sourcebooks, and special bibliographies.

TECHNOLOGY UTILIZATION PUBLICATIONS: Information on technology used by NASA that may be of particular interest in commercial and other non-aerospace applications. Publications include Tech Briefs, Technology Utilization Reports and Notes, and Technology Surveys.

Details on the availability of these publications may be obtained from:

SCIENTIFIC AND TECHNICAL INFORMATION DIVISION

NATIONAL AERONAUTICS AND SPACE ADMINISTRATION

Washington, D.C. 20546